



The phase stability of a VHF meteor trail forward scatter channel and an application : a time synchronization system  
by Daniel Nelson March

A thesis submitted to the Graduate Faculty in partial fulfillment of the requirements for the degree of DOCTOR OF PHILOSOPHY in Electrical Engineering  
Montana State University  
© Copyright by Daniel Nelson March (1966)

Abstract:

The phase stability of 46.55 mhz forward scatter radio reflections from ionized meteor trails is discussed in the first half of the dissertation. The phase stability of the reflections is an indication of the channel length stability and propagation time delay stability. The theory and experimental procedure are developed to determine the phase changes of each received reflection due to the channel.

Data recorded during the school year 1964-65 showed no reflections with phase changes greater than  $10 \times 2\pi$  radian/second. A  $10 \times 2\pi$  radian/second phase shift represents a path length change of 64.2 meter/second or a propagation path time delay change of 0.214  $\mu$ sec/second.

Tests conducted throughout 24 consecutive hours showed that the channel stability remains essentially constant throughout the day. Ho appreciable difference was found in the stability of East-West channels and North-South channels.

The phase variations in the received signals caused by the channel did not indicate the  $2\pi$  radian phase multiplicity between reflections from different principle Fresnel zones. Simultaneous signal paths can exist from either two or more meteor trails or from a single long-lasting trail. The propagation path time delay may be several hundred microseconds different for each path.

Time synchronization systems using the meteor trail reflection channel are the subjects of the second half of the thesis. A manual time synchronization system set a clock in Bozeman, Montana, to within +20  $\mu$ sec of a clock in Seattle, Washington. Operators at both terminals observed reflected pulses from the other terminal on oscilloscopes. An auxilliary voice link was used.

A semi-automated time synchronization system incorporated Polaroid pictures of oscilloscope sweeps displaying a received pulse and a timing waveform. Operators had final control of the clock setting. An auxilliary voice link was again used. Clock synchronization was demonstrated to within several microseconds between Seattle, Washington, and Bozeman, Montana.

The vhf meteor trail forward scatter channel used with the semi-automated time synchronization system was not the limiting factor. The time synchronization system was limited by the simple pulse techniques used.

THE PHASE STABILITY OF A VHF METEOR  
TRAIL FORWARD SCATTER CHANNEL AND AN  
APPLICATION: A TIME SYNCHRONIZATION SYSTEM

by

DANIEL NELSON MARCH

A thesis submitted to the Graduate Faculty in partial  
fulfillment of the requirements for the degree

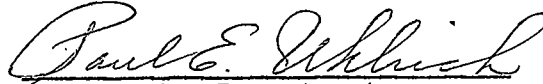
of


DOCTOR OF PHILOSOPHY

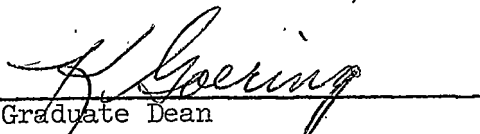
in

Electrical Engineering

Approved:

  
Head, Major Department

  
Chairman, Examining Committee

  
Graduate Dean

MONTANA STATE UNIVERSITY  
Bozeman, Montana

December, 1966

## ACKNOWLEDGMENTS

To Professor Donald K. Weaver, Jr., I express my appreciation and thanks for the thoughtful suggestions and guidance in this research. I also express my thanks to the several graduate students at Montana State University who spent long hours recording and reducing data.

Without the support of The Boeing Company engineers, especially David Albright, Ronald Sanders, and Ernest Manley, the research reported in this thesis would not have been possible. My thanks go to them.

I also wish to thank Dr. William Markowitz, Director of the United States Naval Observatory for his helpful suggestions relative to our time synchronization system.

I want to express my appreciation to the Time and Frequency Division of the National Bureau of Standards, Boulder, Colorado, for their cooperation.

The research reported in this writing was sponsored primarily by The Boeing Company, Seattle, Washington. My thanks to Fred Lightfoot, John Belinski, and Dr. Saturo Tashiro at The Boeing Company for continuing the financial support through the project's completion.

Thanks are also extended to the Montana State University Engineering Experiment Station for financial support.

## TABLE OF CONTENTS

	Page
1.0 INTRODUCTION	1
1.1 History of Radio Reflections from Meteor Trails	2
1.2 Development of Meteor Trail Backscatter Theory	4
1.2.1 Model	4
1.2.2 General Analytic Representation	4
1.2.2.1 Backscatter from Infinitely Long Cylinder	4
1.2.2.2 Backscatter from Underdense Meteor Trails	7
1.2.2.3 Backscatter from Overdense Meteor Trails	12
1.2.2.4 Other Possibilities of Radio Signals from Meteor Trails	13
1.2.3 Work Using Backscatter from Meteor Trails	14
1.3 Background of Forward Scatter from Meteor Trails	14
1.3.1 Historical	14
1.3.2 Forward Scatter Theory	16
1.3.2.1 Contributors	16
1.3.2.2 Underdense Meteor Trail Reflection	16
1.3.2.3 Overdense Meteor Trail Reflections	18
1.4 Meteor Trail Forward Scatter Communication System	19
1.4.1 Basic System Parameters	19
1.4.2 Experimental Communication Systems	20
1.4.2.1 Stanford Research Institute	20
1.4.2.2 Canadian JANET System	21

	Page
1.4.2.3 National Bureau of Standards	22
1.4.3 Developed Communications Systems	22
1.4.3.1 Examples	22
1.4.3.2 System Failures	23
1.4.4 The Seattle, Washington, to Bozeman, Montana, VHF Forward Scatter Link	24
1.4.4.1 History	24
1.4.4.2 Early Tests	24
1.4.4.3 Initial Phase Stability Tests	26
1.4.4.3.1 Equipment	26
1.4.4.3.2 Testing Procedures	26
1.4.4.3.3 Results	27
1.4.4.3.4 A Channel-To-Need Match	28
1.5 Time Synchronization	28
1.5.1 Present Time Synchronization Processes	28
1.5.1.1 General	28
1.5.1.2 Clock Transportation	29
1.5.1.3 Loran C	30
1.5.1.4 Satellite Reflections	30
1.5.2 Limitations	31
1.6 Hypothesis	32
2.0 CHANNEL STABILITY	33
2.1 General Channel Characterization	34

	Page
2.1.1 Model	34
2.1.2 Past Experimental Work	35
2.1.3 VHF Channel Stability	35
2.2 VHF Phase Stability Determination	38
2.2.1 "Double-Doppler" Method	38
2.2.2 Test Configuration	41
2.3 Test Equipment	42
2.3.1 Meteor Trail Forward Scatter Link Tested	42
2.3.2 Derivation of Signals	42
2.3.3 Equipment	43
2.3.4 Quasi-quadrature Functions	46
2.3.5 Calibration	48
3.0 DATA ANALYSIS	50
3.1 Procedure	51
3.1.1 Amplitude Considerations	51
3.1.2 Shape Considerations	51
3.1.3 Signal Phase Changes	53
3.1.4 Examples	54
3.1.4.1 Underdense Meteor Trail Reflection	54
3.1.4.2 Overdense Meteor Trail Reflection	56
3.1.4.3 Non-column Reflection	59
3.2 Other Analysis Considerations	63

	Page
3.2.1 Analysis Problems	63
3.2.2 Rate of Change of Phase	63
3.2.3 Data Reducers	65
4.0 RESULTS OF PHASE STABILITY TESTS	67
4.1 Data Histograms	68
4.2 Numerical Results	68
4.2.1 Worst Case	68
4.2.2 Averages	72
4.3 Early Fast Doppler	73
4.3.1 Nature	73
4.3.2 Explanation	73
4.3.3 Oscilloscope Presentation	78
4.4 24 Hour Test	79
4.4.1 Reasons for Test	79
4.4.2 Data Gathered	79
4.4.3 Results	80
4.4.3.1 Histograms of Hourly Phase Variations	80
4.4.3.2 Histograms of Reflecting Surface Types	84
4.4.3.3 Plot of Percent of Trail Reflections with EFD	86
4.5 Tests Conducted with NBS, Boulder, Colorado	88

	Page
4.5.1 Background	88
4.5.2 Results	92
5.0 INTERPRETATION OF RESULTS	94
5.1 Sudden Changes in Phase Change Rate	95
5.1.1 Test Results	95
5.1.1.1 Apparent Results	95
5.1.1.2 Limitations of CW Signals	95
5.1.2 Causes of Sudden Phase Rate Changes	96
5.1.2.1 Explanation	96
5.1.2.2 Example	99
5.1.3 Phase Plots of Figure 16	100
5.1.4 Observations	104
5.2 Channel Stability Generalities	105
5.2.1 Location	105
5.2.2 Frequency	106
5.2.3 Signal Level	107
5.2.3.1 Transmitted Power and Receiver Sensitivity	107
5.2.3.2 Antennas	107
5.2.4 Path Length	108
5.3 Time Sync Channel Considerations	109
5.4 Summary - Channel Stability	110



	Page
6.0 MANUAL TIME SYNC SYSTEM	113
6.1 Definitions and Assumptions	114
6.2 Equipment	115
6.3 Operation	117
6.3.1 General	117
6.3.2 Example	118
6.3.3 Additional Procedure	121
6.4 Results	122
6.5 Interpretation of Results	124
7.0 SEMI-AUTOMATED TIME SYNCHRONIZATION SYSTEM	127
7.1 Initial Plans	128
7.1.1 Automated Time Sync System	128
7.1.2 Comments by Dr. Markowitz	128
7.1.3 System Solution	129
7.2 Semi-Automated Time Sync System Design	130
7.2.1 Basic Operation	130
7.2.2 Detailed Operation	132
7.2.2.1 Logic	132
7.2.2.2 Timing	134
7.2.2.3 Seattle Terminal	138
7.2.2.4 Synchronization Process	139
7.3 Testing the Semi-Automated Time Sync System	141

	Page
7.3.1 Noise Considerations	141
7.3.2 Time Sync Data	142
7.3.2.1 Limitations	142
7.3.2.2 Results	143
7.4 Interpretation of Results	143
7.4.1 Frequency Difference Errors	143
7.4.2 System Accuracy	146
7.4.3 Channel Errors	147
7.4.4 Proposed Improvements	147
7.5 Concluding Remarks	148
APPENDIX I	151
APPENDIX II	152
LITERATURE CITED	154

LIST OF TABLES

Table	Page
I Summary of Experimental Data	145

## LIST OF FIGURES

Figure		Page
1	Meteor Trail Backscatter Model	5
2	Model Trail Reflected Signal Power	8
3	Meteor Trail Reflection Geometry	17
4	Basic Channel Model	34
5	VHF Meteor Trail Reflection Channel Model	35
6	Coherent Detection of Backscatter	37
7	Quadrature Signal Generation	41
8	Functional Block Diagram of Quadrature Function Receiving System	45
9	Functional Block Diagram of Phase Stability Measuring System	47
10	Detected IF Recording Calibration	49
11	Sample Reflection Types	52
12	Underdense Trail Reflection	55
13	Phase Plot of Underdense Trail Reflection Shown in Figure 12	55
14	Overdense Meteor Trail Reflection	57
15	Phase Plot of Overdense Trail Reflection Shown in Figure 14	58
16	Non-column Reflection	60
17	Phase Plot of Non-column Reflection Shown in Figure 16	61
18	Histogram of 1016 Underdense Meteor Trail Reflections vs. Maximum Phase Shift Rate	69
19	Histogram of 432 Overdense Meteor Trail Reflections vs. Maximum Phase Shift Rate	70

Figure		Page
20	Histogram of 824 Non-column Reflections vs. Maximum Phase Shift Rate	71
21	Reflection With Early Fast Doppler Underdense Meteor Trail	74
22	Plot of Phase vs. Time for Underdense Meteor Trail Reflection Shown in Figure 21	74
23	Cornu Spiral	76
24	Cornu Spiral Axis Projections	77
25	Hourly Histograms of VHF Reflections vs. the Maximum Phase Shift Rate on the Seattle, Washington, to Bozeman, Montana, Forward Scatter Link. Data Obtained March 23-24, 1965	81
26	Histogram of the Diurnal Variation in the Number of Reflections Receiver Per Half Hour From Ionized Meteor Trails and Non-column Surfaces	85
27	Histogram Showing the Diurnal Variation of the Percentage of Meteor Trail Reflections Received With Visible Early Fast Doppler (EFD)	87
28	Histogram of 143 Underdense Meteor Trail Reflections vs. Maximum Phase Shift Rate, Bozeman, Montana, to Boulder, Colorado, March, 1965	89
29	Histogram of 41 Overdense Meteor Trail Reflections vs. Maximum Phase Shift Rate, Bozeman, Montana, to Boulder, Colorado, March 1965	90
30	Histogram of 71 Non-column Reflections vs. Maximum Phase Shift Rate, Bozeman, Montana, to Boulder, Colorado, March 1965	91
31	Propagation Path Geometry for Example	99
32	Possible Phase Plot of Non-column Reflection Shown in Figure 16	101
33	Possible Phase Plot of Non-column Reflection Shown in Figure 16	103

Figure		Page
34	Manual Time Sync Timing Diagram (Slave Clock Ahead)	118
35	Manual Time Sync Timing Diagram (Master Clock Ahead)	120
36	Picture of Repeated Oscilloscope Sweeps Showing Reflected Pulse	123
37	Plot of Measured Error vs. Time of Day	124
38	Block Diagram of Semi-Automated Time Synchronization System	131
39	Delay Timing	135
40	Block Diagram of Timing Waveform Generator	136
41	Nature of Timing Waveform	136
42	Time Synchronization Pictures Taken at Terminals	140
43	Deviation of Data Points	144
44	Circuit Diagram of Pulse Recognition Circuit	152
45	Circuit Diagram of Timing Waveform Generator	153

## ABSTRACT

The phase stability of 46.55 mhz forward scatter radio reflections from ionized meteor trails is discussed in the first half of the dissertation. The phase stability of the reflections is an indication of the channel length stability and propagation time delay stability. The theory and experimental procedure are developed to determine the phase changes of each received reflection due to the channel.

Data recorded during the school year 1964-65 showed no reflections with phase changes greater than  $10 \times 2\pi$  radian/second. A  $10 \times 2\pi$  radian/second phase shift represents a path length change of 64.2 meter/second or a propagation path time delay change of 0.214  $\mu$ sec/second.

Tests conducted throughout 24 consecutive hours showed that the channel stability remains essentially constant throughout the day. No appreciable difference was found in the stability of East-West channels and North-South channels.

The phase variations in the received signals caused by the channel did not indicate the  $2\pi$  radian phase multiplicity between reflections from different principle Fresnel zones. Simultaneous signal paths can exist from either two or more meteor trails or from a single long-lasting trail. The propagation path time delay may be several hundred microseconds different for each path.

Time synchronization systems using the meteor trail reflection channel are the subjects of the second half of the thesis. A manual time synchronization system set a clock in Bozeman, Montana, to within  $\pm 20$   $\mu$ sec of a clock in Seattle, Washington. Operators at both terminals observed reflected pulses from the other terminal on oscilloscopes. An auxilliary voice link was used.

A semi-automated time synchronization system incorporated Polaroid pictures of oscilloscope sweeps displaying a received pulse and a timing waveform. Operators had final control of the clock setting. An auxilliary voice link was again used. Clock synchronization was demonstrated to within several microseconds between Seattle, Washington, and Bozeman, Montana.

The vhf meteor trail forward scatter channel used with the semi-automated time synchronization system was not the limiting factor. The time synchronization system was limited by the simple pulse techniques used.

## 1.0 INTRODUCTION



## 1.0 INTRODUCTION

### 1.1 HISTORY OF RADIO REFLECTIONS FROM METEOR TRAILS

Reflections from the ionosphere were evident with the advent of very high frequency, .30 mhz to 300 mhz, radio transmission in the late 1920's. Engineers soon determined many of the characteristics of these reflections by experimentation. One perplexing problem was, as R. A. Heising<sup>(1)</sup> noted, that some of the sudden changes appeared to be due to "great masses of electrons suddenly tossed into the atmosphere." H. Nagaoka,<sup>(2)</sup> a Japanese engineer, published an article in 1929 discussing the possibility that certain radio disturbances were caused by meteoric showers. However, Mr. Nagaoka had a serious misconception as to what was really happening. He stated that the meteorites were sweeping out the electrons in the ionosphere and this discontinuity was the cause of the abnormal reflections. A. Skellett, J. Schafer, and W. Goodall<sup>(3)</sup> from the Bell Telephone Laboratory conducted radio experiments during meteor showers in 1931 and 1932 and concluded that the changes in the very high frequency, vhf, reflections were directly correlated with the showers. These men realized that the burning meteorites added electrons to the ionosphere and these same men calculated the apparent increase in the electron density. Their work was not, at the time, accepted by most of the radio engineers. By 1936 T. Eckersley<sup>(4)</sup> had determined the heights of the various reflections, the durations, and numbers of reflections per time interval, but he was little concerned as to the phenomena that caused the reflections. Many people soon were working with vhf reflections and useful results were being uncovered. Radio

reflections from ionization left in the E region (80-120 km) by the evaporation (or burning) of meteoroids entering the earth's atmosphere were discussed in several articles<sup>(5,6,7,8)</sup> published in 1938. About this time astronomers were convinced that the reflections were from meteor trails and that they, the astronomers, could learn much from the radio reflections.

World War II stopped most of the specific research relative to radio reflections from meteor trails. However, meteor trail reflections were received on many of the vhf radar sets. Early in the war the reflections caused panic when, as in England, the appearance of similar reflections meant an enemy aircraft or missile. The radar operators soon became familiar with these reflections and discounted their importance. When the war was over, some of the vhf radar equipment was converted specifically for the study of meteor trails. These radars and the technology developed around them showed their applicability to work with meteor trail reflections during the Giacobinid meteor shower which occurred on the night of October 9-10, 1946. The radar sets, many of which had been put into operation just for the shower, were well rewarded with the tremendous number of meteors which were in the shower that night. From such observations in Europe and the United States the potentials of the radar backscatter for study of the meteor trails were obvious<sup>(9,10,11,12,13)</sup>. There were now examples of positive correlation between visual and radio reflection observations of meteors.<sup>(14)</sup> Velocity, height, and other parameters of the meteors (namely those that can be determined by radar measurements) were determined for the shower. In the

group of articles mentioned previously<sup>(9,10,11,12,13)</sup> the authors who were astronomers went on to be the leaders in the area of meteor astronomy while the authors who were engineers became the leaders in the field of vhf reflections from meteor trails. Included in the first group are the Englishmen, Naismith, Prentice, and Lovell; while in the second group are the Americans, Bateman, Pineo, Manning, and Villard and the two Englishmen, Hey and Appleton.

## 1.2 DEVELOPMENT OF METEOR TRAIL BACKSCATTER THEORY

### 1.2.1 MODEL

A model meteor trail<sup>(15,16)</sup> had been assumed by 1948 based on the consideration that ablation of the meteoroid as it entered the earth's atmosphere produced a column of electrons and positively charged ions. A model meteor trail had the following properties: (1) The initial radius of the ionized column was small in comparison to the radio wavelength. (2) The column was stationary in space and not expanding. (3) The charged particles in the trail were not under the influence of recombination or attachment. (4) The trail was infinite in length. (5) The meteor's velocity was considered constant.

### 1.2.2 GENERAL ANALYTIC REPRESENTATION

#### 1.2.2.1 BACKSCATTER FROM INFINITELY LONG CYLINDER

The first analytic representation for the backscatter of vhf waves from meteor trails was done in 1948 by Lovell and Clegg<sup>(17)</sup> at the suggestion of Herlofson. This derivation used the ionized trail model

described above. The basic derivation, as detailed in a more precise form by McKinley<sup>(18)</sup> in 1951, is based on the diagram shown below.

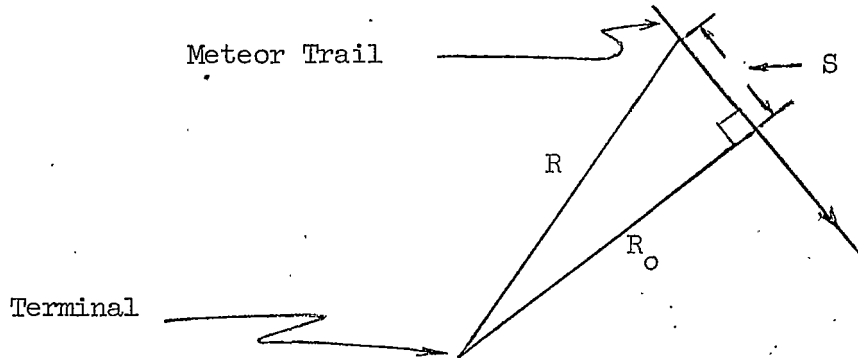


Figure 1.  
Meteor Trail Backscatter Model

From Figure 1:

$$R^2 = R_0^2 + S^2$$

$$\text{and as } S = v(t-t_0)$$

$$R^2 = R_0^2 + v^2(t-t_0)^2 \quad \text{Eq. 1}$$

where  $R$  is the range at time  $t$ ,  $R_0$  is the minimum range at time  $t_0$ , and  $S$  is the distance along the trail measured from  $t_0$ . In this derivation the transmitter and receiver are assumed at the same point with  $\lambda$  the wavelength and  $\omega$  the angular velocity. The amplitude  $A$  and phase of the received electromagnetic wave from a linear element  $ds$  of the line source of electrons in the trail is

$$dA = g(R,q) \sin \left( \omega t - 2 \left( \frac{2\pi}{\lambda} \right) R \right) ds \quad \text{Eq. 2}$$

where  $g(R,q)$  is an amplitude function with  $q$  the line density of electrons.

Historically,  $g(r,q)$  was not derived until after the form of the reflection (that which we are now deriving) was developed. An outline of the  $g(r,q)$  development is given in section 1.2.2.2. It is worthy to note at this time that  $R$  is essentially constant for a given meteor trail as is  $q$ .

To determine the signal contribution from some  $S_1$  to  $S$ , integrate Eq. 2.

$$A_r = g(R,q) \int_{S_1}^S \sin \left( \omega t - 2 \left( \frac{2\pi}{\lambda} \right) R \right) dS$$

To simplify the mathematics, it can be shown that for the region near  $t_0$

$$R = R_0 + \frac{S^2}{2R_0}$$

$$\text{then } A_r = g(R,q) \int_{S_1}^S \sin \left( \omega t - 2 \left( \frac{2\pi}{\lambda} \right) \left( R_0 + \frac{S^2}{2R_0} \right) \right) dS$$

$$\text{Let } \phi = \omega t - 2 \left( \frac{2\pi}{\lambda} \right) R_0 \text{ and } \frac{\pi x^2}{2} = \frac{2\pi S^2}{\lambda R_0}$$

$$\text{then } A_r = \frac{g(R_1,q)(\lambda R_0)^{\frac{1}{2}}}{2} \int_{x_1}^x \sin \left( \phi - \frac{\pi x^2}{2} \right) dx.$$

Then by the conventional Fresnel integrals used in optical diffraction theory

$$A_r = F_r (C \sin \phi - S \cos \phi) \quad \text{Eq. 3}$$

where  $F_r$ , the field strength constant, is  $g(R,q) \frac{(\lambda R_0)^{\frac{1}{2}}}{2}$

$$\text{and } C = \int_{x_1}^x \cos \frac{\pi x^2}{2} dx \text{ and } S = \int_{x_1}^x \sin \frac{\pi x^2}{2} dx.$$

The functions  $C$  and  $S$  vary slowly in comparison with the radio frequency used. The radio frequency used will be greater than  $10^7$  hz while the frequencies of  $C$  and  $S$  will not exceed  $10^4$  hz. As the reflections from near  $x_1$  and more negative are negligible, the value of  $x_1$  can be minus infinity. The power received into a  $1 \Omega$  load (corresponding to the intensity in optics) is

$$P_r = F_r^2 (C^2 + S^2) \quad \text{Eq. 4}$$

This expression is identical to the optical diffraction pattern produced by a straight edge. It represents a steadily increasing power up to the  $t_0$  point (corresponding to the region inside the geometrical shadow in optics), after which the power oscillates about a final average value. The reflections from the Fresnel zones prior to  $t_0$  produce a steadily increasing signal power level. The principal Fresnel zone (PFZ) whose center is at  $t_0$ , increases the power level considerably. The additional Fresnel zones formed after the PFZ produce low level oscillations which decrease in intensity and increase in frequency (corresponding to the diffraction fringes in the region outside the optical geometrical shadow).

Note Figure 2.

#### 1.2.2.2 BACKSCATTER FROM UNDERDENSE METEOR TRAILS

Several years elapsed before the amplitude function was adequately

derived that explained most of the received signals. The final result was the product of contributions from many researchers with McKinley,<sup>(19)</sup> Kaiser,<sup>(20)</sup> Eshleman,<sup>(21)</sup> and Greenhow<sup>(22)</sup> among the major contributors. The same model was used for the electron trail as described earlier.

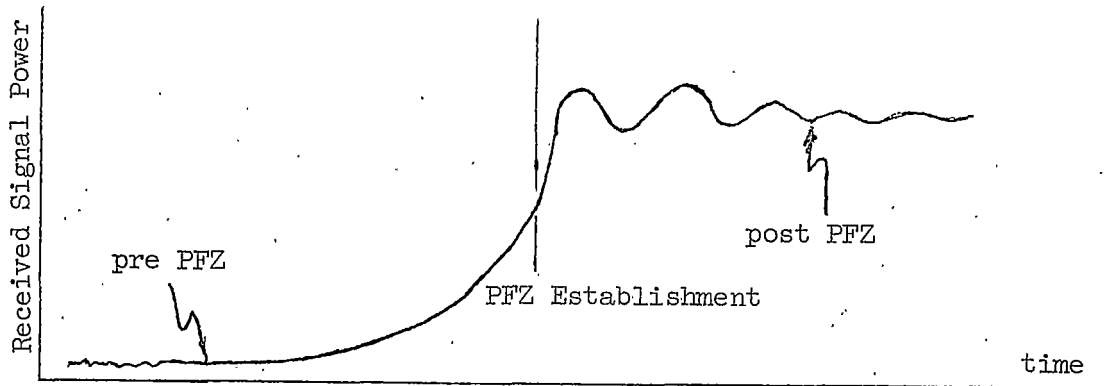


Figure 2.

Model Trail Reflected Signal Power

If the electron density is less than approximately  $10^{14}$   $\text{cm}^{-1}$ , an incident electromagnetic wave penetrates the column. Each electron then oscillates without collisions or other effects (secondary radiative and absorptive effects) from neighboring electrons. The effects from the very much larger and heavier positive ions are neglected. Each electron backscatters as a Hertzian dipole producing an equivalent echoing area

$$\sigma_e = 4\pi r_e^2 \sin^2 \gamma$$

where  $r_e$  is the classical radius of the electron and  $\gamma$  is the angle between the electric vector of the incident wave and the line of sight to the receiver. Note that for backscatter,  $\gamma = 90^\circ$ .

The power flux of the incident electromagnetic wave at the trail is  $\frac{P_T G}{4\pi R^2}$  watts/m<sup>2</sup> where  $P_T$  is the power of the transmitter,  $R$  is the distance between the trail and the transmitter, and  $G$  is the gain of the antenna in that direction relative to an antenna with an isotropic radiating pattern. If the same antenna is used to receive the reflected signal, the effective absorbing area of the antenna is  $G\lambda^2/4\pi$  when matched to the receiver input impedance. Hence the power into the receiver from a single trail electron will be

$$\Delta P_r = \frac{P_T G}{4\pi R^2} \cdot \frac{\sigma_e}{4\pi R^2} \cdot \frac{G\lambda^2}{4\pi} = \frac{P_T G^2 \lambda^2 \sigma_e}{(4\pi)^3 R^4}$$

As all the electrons in each  $ds$  of the trail scatter in phase, the field vectors must be added rather than their power fluxes (note eq. 2). The peak amplitude of the field vector received due to a single electron in the trail is  $(2\Omega\Delta P_r)^{\frac{1}{2}}$  where  $\Omega$  is the receiver input impedance. Now, to consider all the electrons, the field strength is simply multiplied by  $q$ . Thus  $(2\Omega\Delta P_r)^{\frac{1}{2}}q$  is the factor  $g(R,q)$  introduced in eq. 2. Then

$$g(R,q) = (2\Omega\Delta P_r)^{\frac{1}{2}}q$$

and eq. 3 becomes 
$$A_r = (2\Omega\Delta P_r)^{\frac{1}{2}}q \frac{(\lambda R_o)^{\frac{1}{2}}}{2} (C \sin \phi - S \cos \phi)$$

$$\begin{aligned} \text{Now } P_r &= \frac{A_r^2}{2\Omega} = \frac{\Delta P_r q^2 \lambda R_o}{4} [C^2 + S^2] \\ &= \frac{P_T G^2 \lambda^3 \sigma_e q^2}{128 \pi^3 R_o^3} \left[ \frac{C^2 + S^2}{2} \right] \end{aligned}$$



$$= 2.5 \times 10^{-32} P_T G^2 \left( \frac{\lambda}{R_0} \right)^3 q^2 \left[ \frac{C^2 + S^2}{2} \right] \quad \text{Eq. 5}$$

watts

Equation 5 is equation 4 with  $g(R,q)$  evaluated and equation 5 is also the basic equation for the backscatter power received from a meteor trail with an electron density of less than approximately  $10^{14}/\text{cm}^3$ .<sup>\*</sup> Such a trail is called an underdense trail.

However, those working on the amplitude function realized that the total solution was not complete once the amplitude function was evaluated. The ionized trail did not fit the model assumed. The reflections were not totally defined by equation 5. The trail had an initial radius and immediately began to expand due to ambipolar diffusion. As the radius expanded, the electrons on the far side from the transmitter-receiver site began to scatter out-of-phase. Soon the radius was large enough so the net power received from a reflection was nearly zero. The men who derived the amplitude function were aware of this problem and were among those responsible in the early 1950's for the solution. Credit is given to Herlofson,<sup>(23)</sup> Huxley,<sup>(24)</sup> Kaiser and Greenhow,<sup>(25)</sup> and Hawkins.<sup>(26)</sup>

The derivation of the mathematical terms describing the signal level reflected from an underdense trail after it has been formed will be only mentioned as it is not germane to the topic. The derivation is based on the standard form of the radial diffusion equation. To

---

\* Limits on this electron density range from  $10^{12}/\text{m}^3$  to  $2 \times 10^{14}/\text{m}^3$ . The value  $10^{14}/\text{m}^3$  is most often used as the transition density.

apply this, the distribution of electrons around the axis must be known or assumed. Those initially deriving the relations had to assume a distribution. The Gaussian distribution produced results most like those found by experimentation. It has since been shown to be a valid assumption. (27,28) The transformations and integrations which are needed in the derivation are complex. The interested reader is referred to Eshleman (21) and Brysk. (29) The final result is:

$$\frac{P_r(t)}{P_r(0)} = e^{-\left\{\frac{32\pi^2 Dt}{\lambda^2}\right\}} e^{-\left(8\pi^2 r_0^2 / \lambda^2\right)} \quad \text{Eq. 6}$$

where  $P_r(t)$  is power received at time after  $t_0$ ,  $P_r(0)$  is the power received at time equal  $t_0$  by eq. 5,  $D$  is the ionic diffusion coefficient and  $r_0$  is the initial radius. The first exponential in eq. 6 is a function of time and at  $t = 0$ , it is equal to 1. The other term is a constant dependent on the initial radius of the trail and the wavelength. This latter factor will reduce the amplitude function at time  $t_0$  and afterwards. The first exponential has no effect at  $t_0$  but produces an exponential decay after  $t_0$ . The decay time  $T_D$  for meteor trail reflections is that time required for the signal level to fall to  $e^{-2}$  times its value at  $t = t_0$ , or 8.7 db below its initial value. Thus

$$T_D = \frac{\lambda^2}{16\pi^2 D} \quad \text{for underdense trails.} \quad \text{Eq. 7}$$

The decay time is a function of only  $\lambda$  and  $D$ . Such factors as the transmitter power, antenna gain, electron density in the trail, and  $R$  have no effect on  $T_D$ . These factors do, however, affect the initial

received amplitude.

### 1.2.2.3 BACKSCATTER FROM OVERDENSE METEOR TRAILS

The theory for the underdense meteor trail reflections explained many of the reflections received using vhf backscatter. However, there was another class of reflections that it did not explain. These reflections were from overdense meteor trails, those trails with more than  $10^{14}$  electrons/meter. There is no critical transition from underdense to overdense as the  $10^{14}$  electrons per meter implies. This value has been derived as the approximate electron density where the incident electromagnetic wave no longer penetrates the column. In the overdense case, before the incident wave reaches the axis of the trail an electron density is encountered where the refractive index equals zero and hence the wave is reflected. A common analogy is that at that point where  $k = 0$ , a metallic cylinder is encountered. As no electrons on the far side of the trail can produce interference (as the wave doesn't penetrate past the axis) the average overdense trail reflections are higher in amplitude and last longer than the average underdense trail reflection. They do not, however, occur as often.

The theory to explain these reflections was developed after the underdense reflection theory. The two men most responsible for the understanding and theoretical work of the overdense trail reflections were Eshleman<sup>(21)</sup> and Manning,<sup>(30,31)</sup> both from Stanford University. The expression for the amplitude of reflections received from overdense meteor trails is given below.

$$P_r = \frac{G^2 P_t \lambda^2}{64\pi^2 R^3} \left[ 4 Dt \ln \left( \frac{r_e q \lambda^2}{4\pi Dt} \right) \right]^{\frac{1}{2}} \quad \text{Eq. 8}$$

$P_r$  is the amplitude function for a Fresnel integral solution. It applies until the square root term equals zero, then the trail reflection decays exponentially as an underdense trail. In practice this seldom happens. The long lasting (at 50 mc, one or two seconds) overdense trails are blown by the winds to form more than one reflecting area. When this is done the signal components from each reflecting area interfere, destructively and constructively. Hence most reflections from overdense trails are irregular, often with sudden fades and increases in the signal strength. This phenomenon has been investigated extensively. (32,33) No analytic expressions have been derived to indicate this mathematically. The changes are unpredictable except statistically. (34,35)

The theory of the underdense and overdense backscatter reflections will not be elaborated upon here, but will be discussed in detail when needed for later development.

#### 1.2.2.4 OTHER POSSIBILITIES OF RADIO SIGNALS FROM METEOR TRAILS

Some people considered the possibility of reflecting signals off the ionization hypothesized to exist around the meteorite itself. This was shown to be not feasible at moderate power levels due to the extremely small echoing area involved. (36,37) Another possibility considered was that the ablating meteorite or the trail might emit radio signals. After a search for such emissions, Hawkins (37) came to the conclusion that there were no emissions except a slight increase in noise in the vicinity

of 30 mc when a visible meteor was overhead. There was no assurance that this was from radio signals generated by the meteor and not a reflection.

### 1.2.3 WORK USING BACKSCATTER FROM METEOR TRAILS

The radar systems converted to meteor trail backscatter work were used for a great variety of experiments dealing with meteor trails, meteorite physics, meteorite astronomy, and study of the upper atmosphere. Many of these experiments were ingenious, with unique equipment that often became extremely complex. The development of radio techniques gave the meteor astronomers a new research tool. The radio reflection work began in earnest with the Giacobinids shower in 1946 and today new experiments are still being conducted as well as the continuation of long-term studies of certain parameters. The interested reader is referred to A.C.B. Lovell's book<sup>(39)</sup> entitled "Meteor Astronomy" which deals in detail with many radio experiments relative to meteors. For those interested in the relationship between meteors and the ionosphere, the book by Davies<sup>(28)</sup> of NBS covers the subject well. The actual meteoroid environment, in and out of the earth's atmosphere, is the subject of a NASA publication by Cosby and Lyle<sup>(40)</sup> entitled "The Meteoroid Environment and its Effects on Materials and Equipment."

## 1.3 BACKGROUND OF FORWARD SCATTER FROM METEOR TRAILS

### 1.3.1 HISTORICAL

In 1949 and 1950 the articles dealing with radar backscatter from

meteor trails increased as did the knowledge of the reflections. To some clever engineers the possibility of forward scatter from meteor trails became an intriguing possibility. During the initial work with meteor trail reflections, it was noted that the orientation of the trail governed whether a backscatter reflection would be present. A trail whose finite length did not pass through the  $t_0$  point (i.e., such that no perpendicular existed from the trail to the transmitter-receiver site) must still reflect the radio signals, but to some other location. (7,4)

It is impossible to determine who first realized the possibilities of using these "reflections to some other location" for communication. The researchers realized that the area illuminated by each reflection would be limited in size. Hence, if communications were possible, the channel would be somewhat secret. When military men were told of this possibility, they immediately classified the work. Thus, little writing is available relative to the early considerations of forward scatter. By 1950 several experiments were underway to determine the nature of forward scatter reflections. In 1952 several articles appeared in the literature about this work. (41,42) The work showed that not only were signals reflected forward but also they were stronger in amplitude and lasted longer than backscatter reflections. Reciprocity\* was shown to exist between the receiving terminal and the transmitting terminal. (27,42,43) Thus two-way communication was possible. With this newly developed theory the radio engineers proposed to the military that experimental communication links be established. Each of the following organizations developed a

---

\* If terminal A receives terminal B via a meteor trail reflection, likewise B can receive A if the transmitter and receiver are exchanged.

vhf forward scatter link: Stanford Research Institute,<sup>(44)</sup> the National Bureau of Standards,<sup>(45)</sup> and the Radio Physics Laboratory of the Defense Research Board in Canada.<sup>(46)</sup> In 1955 preliminary results were published.

### 1.3.2 FORWARD SCATTER THEORY

#### 1.3.2.1 CONTRIBUTORS

Major contributors to the vhf forward scatter theory were Eshleman,<sup>(21,43)</sup> Manning,<sup>(42,47,48)</sup> and Villard<sup>(49)</sup> at Stanford University and Forsyth, Vogan, and Hines<sup>(46,50,51,52)</sup> of the Canadian Radio Physics Lab.

#### 1.3.2.2 UNDERDENSE METEOR TRAIL REFLECTION

Forward scatter from an underdense meteor trail can be visualized with a model. As with backscatter the line charge of electrons was assumed. The electromagnetic (EM) wave passing through the trail caused each electron to vibrate independently. When the EM wave was not perpendicular to the trail, the  $\sin^2 \gamma^*$  term had to be reinserted to account for the field produced by each Hertzian dipole. The EM wave made an angle of  $\gamma$  with the trail. Addition of the many dipole fields caused the reradiated EM wave to leave the trail at an angle  $180^\circ - \gamma$ . Thus the reflection was specular.\*\* In three dimensional space a line reradiating an EM wave had no single line defined for the reradiation to follow. Thus the reradiation was in the form of a cone which made an angle  $\gamma$  with the trail. The trail was the cone axis. The Fresnel zones were

---

\* Note page 7.

\*\* The angle of reflection is equal to the angle of incidence.

wider with forward scatter than with backscatter. This produced a higher signal level and a slower decay time. The derivation of the amplitude function followed the same principle as that used for the backscatter case. The formula for the power received (according to McKinley<sup>(53)</sup>) at some forward point a distance  $R_2$  from the trail was

$$P_R = \frac{P_T G_T G_R \lambda^3 \sigma_e}{64\pi^3} \frac{q^2 \sin^2 \gamma}{(R_1 R_2)(R_1 + R_2)(1 - \sin^2 \phi \cos^2 \beta)} \quad \text{Eq. 9}$$

with  $P_T$  the power transmitted,  $G_T$  and  $G_R$  the gains of the transmitting and receiving antennas respectively,  $\lambda$  the wavelength,  $q$  the electron density,  $R_1$  the distance from transmitter to trail,  $\phi$  one-half the forward scatter angle and  $\beta$  the angle between the trail and the line of intersection of the propagation plane and the tangent plane. Note Figure 3.

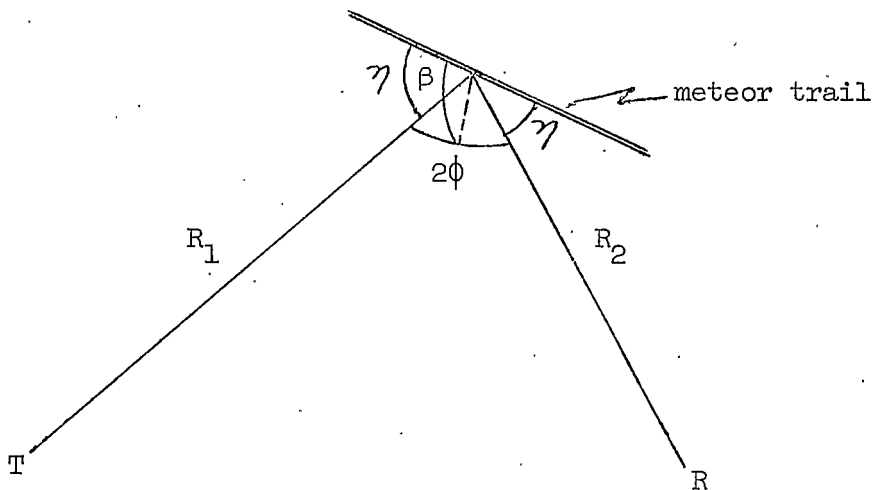


Figure 3.

Meteor Trail Reflection Geometry



The effects of the initial trail radius and its expansion was found by substituting  $\lambda \sec \phi^*$  for  $\lambda$  in equation 6. The result was

$$\frac{P_r(t)}{P_r(0)} = e^{-\left\{\frac{32\pi^2 Dt}{\lambda^2 \sec^2 \phi}\right\}} e^{-\left\{\frac{8\pi^2 r_o^2}{\lambda^2 \sec^2 \phi}\right\}} \quad \text{Eq. 10}$$

Thus the initial trail radius,  $r_o$ , reduced the power by  $e^{-\left\{\frac{8\pi^2 r_o^2}{\lambda^2 \sec^2 \phi}\right\}}$

The  $\sec^2 \phi$  term raised the amplitude compared to the backscatter case.

The decay time was changed to

$$T_D = \frac{\lambda^2 \sec^2 \phi}{16\pi^2 D}$$

The  $\sec^2 \phi$  term lengthened the decay time compared to the backscatter case. (53) The Fresnel integral solution must be added to equation 9 to complete the nature of the signal development.

### 1.3.2.3 OVERDENSE METEOR TRAIL REFLECTIONS

The forward scatter reflections from overdense meteor trails were more difficult to characterize mathematically. Considerable work was done in an effort to explain them. (48,52) The reflections from such trails were so varied in form that the best that could be done was a statistical analysis. The winds were the primary cause of the irregular signals from the long lasting trails.

---

\* For a meteor trail 100 km above the midpoint between two stations 400 km apart  $\sec^2 \phi$  is approximately 5. If the two stations are 1000 km apart  $\sec^2 \phi$  is approximately 25.

## 1.4 METEOR TRAIL FORWARD SCATTER COMMUNICATION SYSTEMS

### 1.4.1 BASIC SYSTEM PARAMETERS

Reflections from underdense and overdense meteor trails were intriguing to the radio communication engineers because; (1) they permitted long range (1500 miles) communications at frequencies otherwise unusable, (2) the equipment needed was standard except for burst nature of channel, (3) high signal-to-noise ratios and wide bandwidths were available at moderate power levels, and (4) there appeared to be some secrecy to the channel. There were also several problems, namely: (1) the signals were only intermittent, (2) the duty cycle was low, (3) the occurrences of the reflections were only predictable statistically. The latter areas did not present themselves as insoluble problems to the engineers at the Stanford Research Institute (SRI), NBS, and the Radio Physics Lab in Canada that developed communication links using the meteor trail reflections as the data channel. Each system solved the problems just mentioned in much the same manner; all used the basic solutions proposed by the Stanford University engineers.<sup>(42,43)</sup> The solutions to the problems were (1) as the signals were intermittent, data was transmitted only when a reflecting surface permitted communications, (2) due to the low duty cycle data were simply transmitted at a high rate whenever a reflecting surface was available, (e.g. if the duty cycle was 10%, then the average data rate desired was increased by a factor of 10 during transmissions) and, (3) the channel was sampled at frequent intervals (each 10 msec.) to determine when a reflecting surface existed between the two stations.

## 1.4.2 EXPERIMENTAL COMMUNICATION SYSTEMS

## 1.4.2.1 STANFORD RESEARCH INSTITUTE

The SRI link<sup>(44,54)</sup> operated between Palo Alto, California, and Bozeman, Montana, a distance of 820 miles. This was not a bilateral system as information could only be sent from Bozeman to Palo Alto. At Bozeman a 2 kw cw signal at 40.38 mhz fed a 3-element Yagi antenna. When the signal was received at Palo Alto, a return signal was sent from Palo Alto at 30.80 mhz (again at a 2 kw power level) to Bozeman which said essentially, "We are receiving your signals, transmit data." At Bozeman the cw mode was changed to data when this signal was received. Teletype was sent with the data rate increased by a factor of 10. An FSK modulation was used. The information continued to be sent until another signal was received from Palo Alto which said essentially, "Send no more data till Palo Alto asks for more." This instruction from Palo Alto was sent if: (1) the signal received from Bozeman fell below a given threshold, (2) the receiving storage was filled, or (3) there was an equipment malfunction at the Palo Alto receiving site. The Bozeman transmitter then returned to cw operation and the process was repeated with the next reflection. Two types of data storage units were tested, one a magnetic tape unit and the other a magnetic core storage unit. Both operated satisfactorily. Voice was also transmitted over the channel in a series of tests.

SRI personnel were impressed with the operation of the communication system. In the December, 1957, proceedings of the Institute of Radio Engineers, the SRI engineers said, "Operation of this system to date has

definitely proved the feasibility of long range vhf communications via meteor-reflected signals."<sup>(44)</sup>

#### 1.4.2.2 CANADIAN JANET SYSTEM

The meteor trail reflection work at Stanford and SRI was given the name "meteor-burst." The Canadian\* vhf link was given the code name JANET, "After Janus, the Roman god of the doorway who looked both ways at once."<sup>(46)</sup> The JANET system operated on a bilateral basis, i.e., information was transmitted and received at both terminals. Various frequencies were used in the 30-50 mhz range. The information was teletype code with the data rate transformed by a factor of 21.<sup>(55)</sup> Double sideband amplitude modulation was used with approximately 750 watts feeding 5 element Yagi antennas. Magnetic tape storage was used.<sup>(56)</sup> The operation of the system was tested under different configurations of the equipment parameters. The evaluation of the system in the December 1957 Proc. of the IRE was more reserved than was that of the SRI system. The Canadians did feel, however, that the vhf meteor trail reflections constituted a channel that might fulfill the need they had for communications to the sparsely settled north country. They needed "low power, reliable, point-to-point communications for use over ranges of the order of 500 to 1500 km."<sup>(46)</sup> The developers of the JANET system planned to do more testing in an effort to get a usable system.

---

\* Radio Physics Lab, Research Board, Ottawa, Canada.

### 1.4.2.3 NATIONAL BUREAU OF STANDARDS

The National Bureau of Standards conducted a series of experiments involving vhf forward scatter from meteor trails between Cedar Rapids, Iowa, and Sterling, Virginia, which were reported in 1952. This report appeared favorable to those who were considering meteor trail forward scatter for long range communications. (45,46,57) NBS also thought the system should be investigated further. After several years of work, a communications link with a great circle distance of 1277 km was set up from Kilbourne, Illinois, to Erie, Colorado. The frequencies used were both near 50 mhz with one-half mhz separation. Magnetic tapes were used for data speed translations. Ten, 20, 40, and 80 times normal teletype speeds were available. Several reports were written about the work indicating that reasonable error rates were achieved and, in general, favorable results were indicated. (57,58,59)

### 1.4.3 DEVELOPED COMMUNICATIONS SYSTEMS

#### 1.4.3.1 EXAMPLES

The accounts of the trial meteor trail forward scatter systems aroused the interest of both communications engineers and military personnel. The military wanted a wideband vhf long range communication system. The secrecy aspects of the channel were even more appealing. Soon both the Air Force and Navy had awarded developmental contracts.

As work developed on these systems Bozeman was again chosen as one terminal for three of the links. The Electronics Research Laboratory operated the remote terminal for Hughes Aircraft when they tested their ground-to-ground system and their ground-to-air link. The Hoffman

Electronics link was found to be inoperative due to poor equipment design. To eliminate this factor, the Air Force asked the ERL to put the equipment in an operational state. The malfunctions were corrected and the system was tested. Another company to choose Bozeman as the second terminal was The Boeing Company. Again the ERL operated the equipment during the testing phases.

#### 1.4.3.2 SYSTEM FAILURES

These systems did not perform as well as the engineers had anticipated. None of the systems developed was able to fulfill the established requirements. The basic problem in each case was simply that the duty cycle was not high enough to permit transfer of a reasonable amount of data in a specified time. To the people who had to deliver a usable product to a discriminating sponsor, the channel appeared more limited than it had to the initial investigators. It was said that when the developed command system was demonstrated to a high military commander, he pushed the "fire" button and nothing happened for fifteen minutes. The commander was outraged and demanded to know what had happened. It was explained that there was no guarantee a meteor trail that was properly oriented to reflect signals between two points would exist in any specified time interval.\* The meteor trail forward scatter link was rejected for the command system and the other uses that had been proposed for it. By 1960 the Air Force had decided that too many millions had been spent on the idea with no useful results. The Navy was also

---

\* The author has seen periods of nearly an hour between reflections on the Seattle, Washington, to Bozeman, Montana, vhf link.

disenchanted but did continue with some in-house experimentation. Hence in 1960 essentially all government support for meteor trail forward scatter communication systems was terminated.

#### 1.4.4 THE SEATTLE, WASHINGTON, TO BOZEMAN, MONTANA, VHF FORWARD SCATTER LINK

##### 1.4.4.1 HISTORY

The Boeing Company, unlike the other companies working in the field, had not had government support for their work. However, in 1960, it was apparent that their system was working no better than the others. The ERL personnel suggested to Boeing that additional testing be conducted on the Seattle-Bozeman channel. The link was well equipped with transmitters, antennas, and receivers. ERL personnel felt that the channel with its unique parameters would be the answer to some equally unique communication problems. Before such a channel-to-need match could be found, experimentation was needed to more adequately define the channel parameters.

##### 1.4.4.2 EARLY TESTS

In the three-year interval between 1960 and 1963, tests were conducted\* on the 46.55 mhz link between Seattle, Washington, and Bozeman, Montana, a great circle route distance of 880 km. The power received at the terminals was checked against the theoretical power level (eq. 9). Close agreement was found. The following parameters were determined for

---

\* Credit must be given to Dr. D. K. Weaver and Mr. E. Molthen at the ERL who suggested the work and to Messrs. John Belenski and Fred Lightfoot for their enthusiasm and support at the Boeing Company.

the channel; the duty cycle above present thresholds, the distribution of reflection durations above given present thresholds, and daily and seasonal variations. Not all of the results were in agreement with theory or with earlier test results obtained by other organizations. It was found that the diurnal variations were not as great as those predicted by theory or found in earlier testing. Tests to determine channel reciprocity were conducted. The channel defined by underdense meteor trail reflections was found to be approximately 90% reciprocal.\* No conclusions were made relative to the overdense meteor trail reflection channel reciprocity. Modulation tests were conducted to determine threshold settings; multipath distortions, and the effects of severe fading conditions. The tests and results were detailed in the Boeing document No. D2-20788 entitled "Meteor Burst Communication Research Program."<sup>(60)</sup>

A series of modulation tests showed that more information had to be known about the stability\*\* of the vhf reflections from meteor trails. If a coherent modulation was used, the data waveshapes had to exist in time long enough so that channel perturbations did not render the waveform unrecognizable. Note that for meteor trail reflections a threshold could be pre-set such that a high signal-to-noise ratio was present before communications began. Under these circumstances the principle

---

\* When a vhf signal could be propagated from Bozeman to Seattle, 90% of the time a signal could be propagated to Seattle to Bozeman.

\*\* By "stability of the reflection" was meant the stability of the path length with respect to time during the reflection; or, equivalently, the stability of the position of the equivalent reflecting point on the meteor trail; or, equivalently the changes in the phase of the received signal caused by the meteor trail reflection channel.



factor that could distort the waveform was large phase changes in the signal due to the channel.

#### 1.4.4.3 INITIAL PHASE STABILITY TESTS

##### 1.4.4.3.1 EQUIPMENT

To initially check this "phase stability" of the channel, a simple test was conducted on the Seattle-Bozeman 46.55 link.\* The Seattle transmitter was turned on for 100  $\mu$ sec each 10 msec. The 10 msec timing was derived from an accurate 1 mhz crystal oscillator while the 100  $\mu$ sec pulses were derived from a one-shot multivibrator. At the Bozeman receiving site an operator observed the receiver 2.25 mhz IF on an oscilloscope. The oscilloscope was triggered each 10 msec with a 100 hz square wave which also was derived from an accurate 1 mhz crystal oscillator.

##### 1.4.4.3.2 TESTING PROCEDURE

If the scope trace had a horizontal sweep of 1 msec/cm, when a reflection occurred the received pulses would appear some place on the scope face. If the reflection lasted for 200 msec then there would be 20 sweeps across the scope face during that time. Each sweep would show the received pulse in approximately the same position. After several reflections, the operator would notice that each reflection produced pulses that were displayed on the same area on the scope face,  $\pm 500 \mu$ sec. The operator would then shift the 100 hz triggering square wave such that the scope sweep began just before the time interval containing most

---

\* Credit is due Mr. C. P. Edwards and Mr. A. Bradley for this work.

of the reflected pulses. The sweep velocity would then be changed until the interval containing the pulses covered the scope face. This meant that the sweep rate was usually at 100  $\mu\text{sec}/\text{cm}$ . A camera was mounted on the scope face with a shutter that was manually opened and closed. The operator could see the scope face through the camera mounting. He would open the shutter when a pulse was seen on the scope. As soon as the pulses disappeared or before, the shutter would be closed. This process produced a picture of consecutive sweeps of the scope showing a received pulse on each or at least on most of the sweeps.

#### 1.4.4.3.3 RESULTS

The engineers then studied the pictures to see if there was a measurable change in the position of the pulse. If the 100 hz square waves at both terminals were accurate, changes in the position of the pulses on the picture indicated that the propagation delay time had changed. Many pictures were taken after the operators became sufficiently talented. None of the pictures taken showed changes in the position of the pulses. A few pictures were taken with the scope sweep at 50  $\mu\text{sec}/\text{cm}$  but still no significant position changes were noted. The pulses appeared together on each picture except for slight variations attributed to additive noise. These simple tests showed that the channel had a constant propagation time for each reflection to within a few microseconds. The experiment showed that the channel propagation time delay might be constant to within fractional microsecond limits for each reflection.

#### 1.4.4.3.4 CHANNEL-TO-NEED MATCH

For distant time synchronization\* a communication channel was needed with the following parameters: (1) high signal-to-noise ratios, (2) wide bandwidths, (3) reciprocity, (4) low power levels, and (5) stable propagation times. Tests on the vhf forward scatter link between Seattle and Bozeman had shown the channel possessed the first four parameters. If the vhf link had a propagation time that was constant to within microsecond limits for each reflection, then the channel could be the solution. This would be a channel-to-need match.

### 1.5 TIME SYNCHRONIZATION

#### 1.5.1 PRESENT TIME SYNCHRONIZATION PROCESSES

##### 1.5.1.1 GENERAL

Presently there are several methods available to time synchronize two clocks located far apart. None of the processes use a channel with characteristics listed in section 1.5.4.2. As a result the radio processes used are complex, costly, and often not reliable. In the brief description of time synchronization processes to follow, those processes dealing with astronomy will not be covered. Such methods, in general, are not appropriate for the users considered here; namely, scientific laboratories, the military, and the space agencies. (61)

The oldest radio technique for determining time, which is used where precise accuracy is not needed, involves the recognition of a

---

\* A remote clock must be set so that when a master clock reads 8 o'clock, the remote also reads 8 o'clock within some error limits.

particular keyed tone on one of the National Bureau of Standards' timing frequencies of 5, 10, 15 or 20 mhz.<sup>(62)</sup> The propagation time cannot be calculated precisely but an estimate can be made. Accuracies expected are not better than several milliseconds. As simple antennas and receivers are usually sufficient to receive the signal well, the process is simple and economical but not extremely accurate.

#### 1.5.1.2 CLOCK TRANSPORTATION

To achieve time synchronization to within a few microseconds, a stable clock can be set with the primary clock and carried to the remote clock for synchronization. Either a quartz crystal oscillator and clock are transported or an atomic resonance frequency standard with clock is transported. The crystal-controlled clocks have been transported extensively by NASA but little has been done to determine exactly how accurately the remote clock was set. In June, 1965, the National Bureau of Standards planned to run a series of tests to determine how accurately this could be done. No reports have yet appeared. Initial tests by the Hewlett-Packard Company in conjunction with the Naval Observatory indicated that a cesium standard and clock could be transported long distances and yet maintain accurate time.\*<sup>(63)</sup> However, these clocks are expensive and good transportation facilities must be available throughout the clock's journey. The Navy cannot consider transporting such a clock to several ships. The transporting also takes considerable time. The Electronics Research Lab planned in 1965 to use

---

\* In a trip around the world the clock's accuracy was maintained to within one microsecond of the Naval Observatory time.<sup>(64)</sup>

one of these clocks for a time synchronization procedure between NBS at Boulder, Colorado, the ERL in Bozeman, Montana, and The Boeing Company in Seattle, Washington. To rent such a clock so that each location would be synchronized involved a sum of nearly \$5,000. This did not include transportation costs. The test has not been conducted.

#### 1.5.1.3 LORAN-C

The Loran-C navigation and timing system uses three vlf transmitting stations located some distance apart.<sup>(65,66)</sup> Each of these stations transmits pulses which are synchronized in time to the other stations. At a distant receiver, the time differences between the received pulses allow the operator to triangulate, using hyperbolas, to determine its location. Once the remote station knows its location it can calculate the propagation time from one of the Loran-C stations to itself. Knowing this, it can then locate a particular axis crossing of the received vlf wave from that station which is synchronized to the U.S. Naval Observatory time. With this information it is possible to calculate the time at the receiver. Accuracies over water have been claimed to plus or minus a micro-second but extensive data have not been taken. Over land, where the propagation time is less predictable, the timing is correspondingly less accurate.<sup>(66)</sup> A remote station must, of course, be in an area where the signals are received with a high signal-to-noise ratio.

#### 1.5.1.4 SATELLITE REFLECTIONS

The U.S. Naval Observatory has developed a time synchronization

method using the Relay satellite. During a visit to the Montana State University campus in the spring of 1965, Dr. Wm. Markowitz, Director of Time Services, U.S. Naval Observatory, presented a seminar on this system. The system described was tested between California and Japan. The time synchronization accuracies were within one or two microseconds. Dr. Markowitz thought that the accuracies could be improved. This technique probably will not be the solution for the majority of the organizations needing time synchronization. High transmitter powers and large antennas are needed due to the satellite height and the low signal levels from the satellite. Also, as the satellite is continually moving, the path length between the two stations via the satellite is continually changing in length. The effects of the changing propagation time must be considered. To account for this it was necessary to use a computer. Unless reductions in the equipment complexity are possible, this method of time synchronization will be practical only between primary time standards.

#### 1.5.2 LIMITATIONS

Each of the time synchronization processes mentioned above have limitations. There is still a class of users that have no practical means of time synchronization. Previously, as more accurate time-keeping has become economically available, the scientific and commercial users have expanded their operations to use this additional timing accuracy. (61, 67, 68) The development of a simple time synchronization system that is not economically or transportation limited, yet accurate and reliable will not only fulfill a present need but will give the scientific and commercial

communities another valuable tool. The vhf meteor trail forward scatter channel may allow such a time synchronization system to be built.

#### 1.6 HYPOTHESIS

The working hypothesis guiding this investigation is twofold. First, the communication channel defined by vhf radio signals reflected from ionized meteor trails is stable during each reflection. Second, a time synchronization system can be designed, constructed and tested that uses the vhf meteor trail forward scatter channel which can synchronize two clocks to within +1  $\mu$ sec.

## 2.0 CHANNEL STABILITY



## 2.0 CHANNEL STABILITY

## 2.1 GENERAL CHANNEL CHARACTERIZATION

## 2.1.1 MODEL

A narrowband communication channel can be characterized with a series combination of an attenuator, a time delay, and additive noise.

Note Figure 4. (69,70)

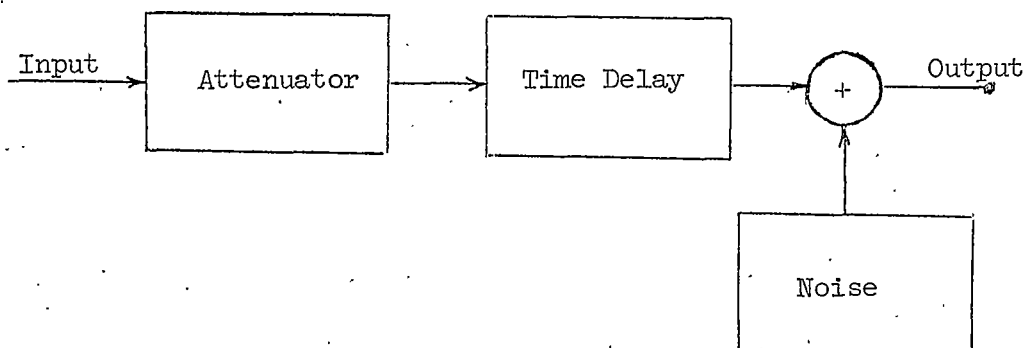


Figure 4.

Basic Channel Model

A signal transmitted through the channel has its amplitude changed by the attenuator (which could be an amplifier) and is delayed in time by the time delay (which cannot be negative). Without loss of generality all of the channel noise is considered additive. (28,71) To simulate the meteor trail forward scatter channel the attenuator is a dynamic element. With no reflection present the attenuator setting is near infinite. A reflecting meteor trail Fresnel zone causes the attenuator to change to a value such that the signal power out is that defined by equations 9 and 10. After this level is established, the attenuator will change to produce an exponential decay of the signal level if the trail is underdense (equation 11). If the meteor trail is overdense the attenuator settings are defined only statistically as are the signals themselves.

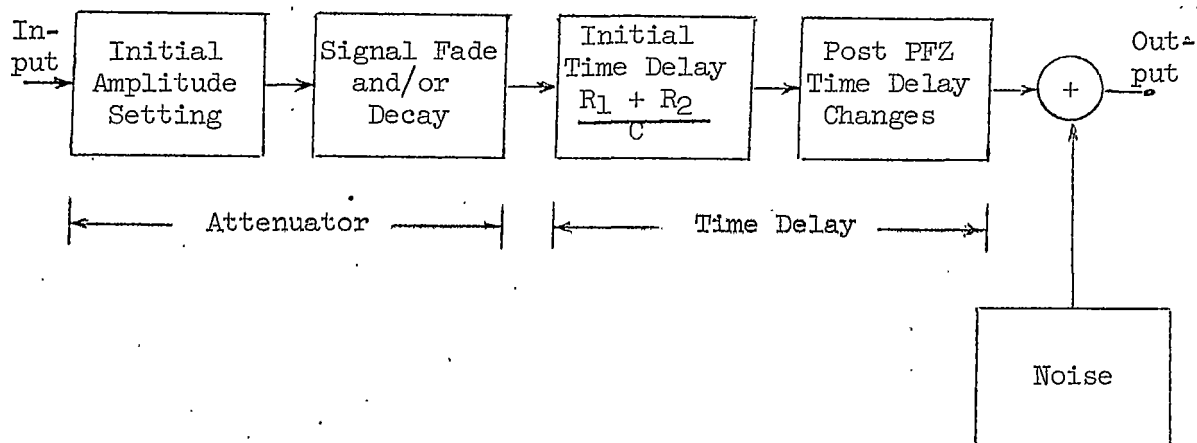


Figure 5.

## VHF Meteor Trail Reflection Channel Model

## 2.1.2 PAST EXPERIMENTAL WORK

The nature of the amplitude of received vhf meteor trail reflections has been studied and experimentally verified for many forward scatter links<sup>(74)</sup> including the one established on 46.55 mhz between Seattle, Washington and Bozeman, Montana.<sup>(60)</sup> Time delay variations between reflections on a vhf forward scatter link have been investigated by NBS.<sup>(75)</sup> Limited data relative to this have been gathered for the Seattle-Bozeman link. Little work has been done to determine the true propagation time. No published theory or experimental work has been found relative to the changes in time delay after the signal has established itself (after the principle Fresnel zone). This is the channel parameter which was investigated in part (1) of the hypothesis.

## 2.1.3 VHF CHANNEL STABILITY

If the signal transmitted on the channel is a vhf signal, what effect

does a small change in the delay have on the signal? If a cw signal is transmitted, a phase change will occur when the time delay is increased by  $\Delta t$ . The cw signal will be received after the  $\Delta t$  increase in delay, but the phase of the signal is retarded by

$$2\pi \frac{\Delta t}{\left(\frac{1}{f}\right)} \quad \text{radians}$$

where  $f$  is the frequency. To measure the  $\Delta t$  delay translation or the corresponding change in phase of the signal, a comparison must be made of the received signal with either the transmitted signal or its reconstruction. Radio astronomers studying meteors and engineers studying upper atmospheric winds use the first procedure extensively.\* They locate their receiving site a short distance from the transmitter in a null zone of the transmitting antenna radiation pattern. The location is chosen so that the ground wave from the transmitter is received but not enough to saturate the receivers. A cw vhf signal is transmitted. When a reflection is received at the receiving site the receiver output is the sum of the reflection and the ground wave. As the phase of the reflection changes relative to the ground wave, the net signal strength changes from the sum of the two signals, when they are in phase, to the difference when they are out of phase. If the receiver IF is detected, the detector output is  $\sin \Delta\phi$  where  $\Delta\phi$  is the phase shift between the two signals. This coherent detection of the backscatter from a meteor trail produces a signal as shown in Figure 6 below (the PFZ is assumed stationary).

---

\* Manning, Villard, and Peterson of Stanford<sup>(77)</sup> and McKinley in Canada<sup>(76)</sup> developed this process.

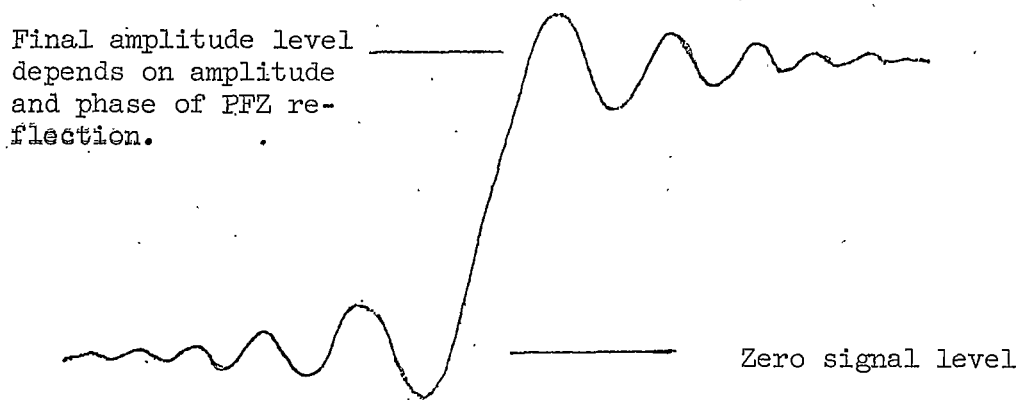


Figure 6

## Coherent Detection of Backscatter

The oscillations before the PFZ are caused by phase changes of the backscatter signal caused by each additional Fresnel zone formed by the meteor. These oscillations have a one-to-one relation with the C and S terms in Equation 3. The oscillations superimposed on the post-PFZ signal are likewise related to C and S. To measure the meteor's velocity, knowing its distance from the transmit-receive site,\* the engineers measure the time taken by the received signal to change phase a given amount ( $\phi_1 - \phi_2$ ). The phase change represents a distance along the meteor's path. The velocity is then simply  $ds/dt$ , where  $ds$  is the path length traversed between the phase limits and  $dt$  is the time required for phase to change from  $\phi_1$  to  $\phi_2$ .

---

\*. Researchers determine the distance to the meteor trail with either an auxiliary radar unit or by incorporating radar techniques into the transmitted signal.

The oscillations before the PFZ represent a shortening path length. The phase changes before the PFZ are nearly linear functions of time as the pre-PFZ Fresnel zones are nearly the same length and the meteor's velocity changes little<sup>(77)</sup> while forming the trail. This produces a pre-PFZ signal high in frequency by the frequency of the pre-PFZ oscillations (Doppler theory). The meteor velocities determined with this method are in good agreement with visual and radar measurements.

To those that developed the process there were some anomalies noted that were not explained by theory. The slow changes in phase of many of the received signals prompted the Stanford group to devise their "Double-Doppler Study of Meteoric Echoes."<sup>(78)</sup> This investigation established the study of atmospheric winds using meteor trail vhf backscatter.

## 2.2 VHF PHASE STABILITY DETERMINATION

### 2.2.1 "DOUBLE-DOPPLER" METHOD

The "double-doppler" method of studying the movement of the meteor trail's effective reflecting point will be discussed here as the same basic procedure was used to measure the channel stability of the Seattle-Bozeman vhf meteor trail forward scatter link. The Stanford engineers were looking for information relative to the direction of the phase change rather than just the coherent detection of the reflection. This would allow them to determine if the effective reflection point was moving toward or away from the receiver. If a signal is mixed with the reflected wave which is not at the same frequency as the transmitted wave, then the detected output is shown in Equation 12,

$$\sin \omega_1 t \sin (\omega_0 t + \phi(t)) = \sin [\omega_0 t - \omega_1 t + \phi(t)] \quad \text{Eq. 12}$$

where  $\omega_0 t$ , the transmitted radian frequency, is higher than the mixing signal  $\omega_1 t$  radian frequency and  $\phi(t)$  is the phase change of the reflected signal relative to the transmitted wave. Note that the phase change is a function of time also. If both  $\omega_0 t$  and  $\omega_1 t$  are constant in frequency, then their difference is

$$\omega_0 t - \omega_1 t = (\omega_0 - \omega_1)t = \omega_D t$$

where  $\omega_D$  is the difference in radian frequency. Now, if the path length is shortening, the detected output will be  $\sin [\omega_D t + \phi(t)]$  whereas if the path length is lengthening, the output will be  $\sin [\omega_D t - \phi(t)]$ . Similar results are true if  $\omega_1 t > \omega_0 t$ . Thus if the mixing signal is different from the transmitted signal in frequency, it is possible to analyze the detector output to determine if the phase changes,  $\phi(t)$ , are adding or subtracting from  $\omega_D t$ . When using  $\sin \omega_0 t$  to mix with the received reflection and then detecting, this ability to determine the sign of  $\phi(t)$  is lost. The early experimenters might have used this process but they did not have sufficiently stable signal sources for  $\sin \omega_0 t$  and  $\sin \omega_1 t$ . As a result they were forced to devise a procedure using  $\sin \omega_0 t$  as the mixing signal.

The received signal (now considering amplitude as well as phase) can be put into rectangular form as shown below,

$$A(t) \cos [\omega_0 t + \phi(t)] = E_1(t) \cos \omega_0 t + E_2(t) \sin \omega_0 t \quad \text{Eq. 13}$$

where  $A(t)$  is the amplitude function of the received signal. The  $E(t)$  functions contain all the information contained in  $A(t)$  and  $\phi(t)$  as:

$$A^2(t) = E_1^2(t) + E_2^2(t)$$

$$\tan \phi(t) = - \frac{E_2(t)}{E_1(t)}$$

If  $\omega_0$  is the center radian frequency of a signal, then  $E_1(t)$  and  $E_2(t)$  become quadrature functions<sup>(79)</sup> each with half the bandwidth of the original signal.

$$\text{Note that } E_1(t) = A(t) \cos \phi(t) \quad \text{Eq. 14}$$

$$\text{and } E_2(t) = -A(t) \sin \phi(t) \quad \text{Eq. 15}$$

These functions completely describe the amplitude and phase of the received signal. To generate  $A(t) \cos \phi(t)$ , the Stanford engineers mixed  $\sin \omega_0 t$  with the reflected signal and filtered out the high frequency component.  $\sin [\omega_0 t + \pi/2]$  was mixed with the reflected signal to produce the low frequency output  $A(t) \cos[\phi(t) + \pi/2]$ . Then as

$$\cos (B + \pi/2) = - \sin B$$

$$A(t) \cos [\phi(t) + \pi/2] = -A(t) \sin \phi(t).$$

The received signal was mixed with either  $\sin \omega_0 t$  or  $\sin (\omega_0 t + \pi/2)$  in balanced modulators. These were followed by lowpass filters. Note figure 7 below.

If the path length is shortening,  $\phi(t)$  is positive. With  $\phi(t)$  positive, the  $A(t) \cos \phi(t)$  term leads the negative  $A(t) \sin \phi(t)$  term by  $\pi/2$ . If the path length is lengthening,  $\phi(t)$  is negative. The negative  $A(t) \sin \phi(t)$  term then leads  $A(t) \cos \phi(t)$  by  $\pi/2$ .

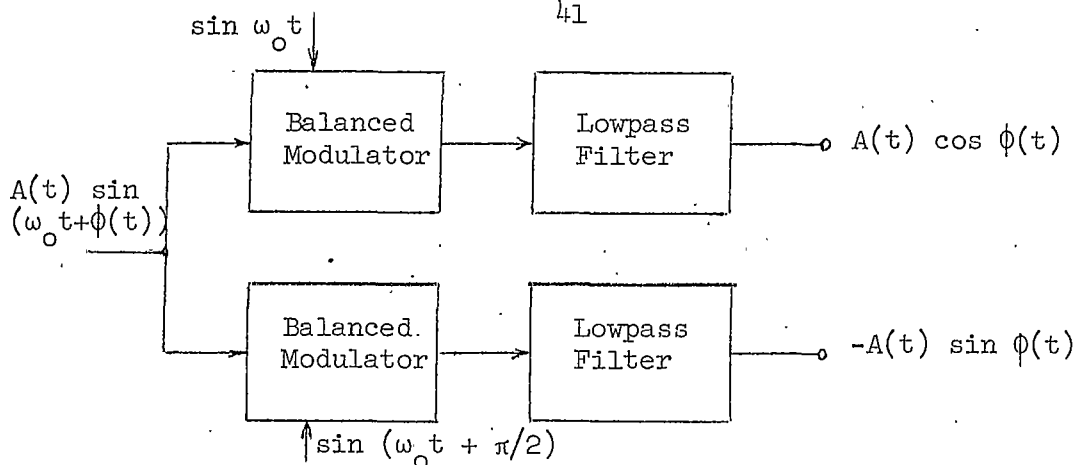


Figure 7.

### Quadrature Signal Generation

The data gathered by the Stanford group showed that after the PFZ the reflection often slowly changed phase, usually at a constant rate. This phase change was so constant that they regarded it as a frequency offset; either positive or negative. This phase shift was named by them "body doppler." After studying the phenomena they deduced that it was caused by upper atmospheric winds<sup>(78)</sup> moving the trail at a constant rate. The work also showed that the sudden fades in long-lasting signals were the result of the beating of two or more components of reflected signal, the "glint" theory.<sup>(78,80)</sup>

#### 2.2.2 TEST CONFIGURATION

To extend this testing procedure to meteor trail forward scatter, the transmitted frequency had to be accurately reconstructed at the receiving site. With the advent of stable crystal oscillators phase-compared to WWVL and stable frequency synthesizers, this process was practical. Thus the test that was proposed to The Boeing Company was essentially that test outlined in D. K. Weaver's thesis,<sup>(79)</sup> "Quadrature



Signal Functions and Application."

## 2.3 TEST EQUIPMENT

### 2.3.1 METEOR TRAIL FORWARD SCATTER LINK TESTED

The vhf meteor trail forward scatter phase stability tests were conducted on the 46.55 mhz link between the MSU Electronics Research Laboratory field site one-half mile south of the campus and a Boeing Company field site near Seattle, Washington. The geographic positions of the two stations were Lat. 45 39 28 N; Long. 111 02 59 W and Lat. 47 37 23 N; Long. 122 01 38 W, respectively. The Boeing Company field site was the transmitting terminal with all receiving, recording, and data analysis at the Bozeman terminal. This is the same link that was extensively tested during 1961, 1962 and 1963. The original 46.55 mhz Seattle transmitter was used. The antennas used for the phase stability measurements at both terminals had been also used for earlier tests.

### 2.3.2 DERIVATION OF SIGNALS

To achieve signals of constant and known frequency, precision one mhz crystal frequency standards were installed at both terminals. The frequency standard at the Seattle terminal was phase compared to the 60 khz WWVB station at the National Bureau of Standards in Boulder, Colorado. The 60 khz signal transmitted there is maintained accurate to within  $\pm 2$  parts in  $10^{11}$ . By phase comparing a signal derived from the standard to the WWVB receiver, the crystal oscillator can be kept

extremely accurate. (62,81) The Seattle standard was maintained accurate to  $\pm 3$  parts in  $10^{10}$ . At the Bozeman terminal the frequency standard was phase compared to a signal from the ERL primary frequency standard. The ERL primary standard, a Hewlett-Packard 103-AR, was phase compared to WWVB. It was maintained accurate to within  $\pm 3$  parts in  $10^{10}$ . A 100 khz signal from the primary standard was transmitted to the field site over a set of direct telephone lines (no amplifiers). At the field site this 100 khz signal was compared to a 100 khz signal from the field site standard in a Montronic's Frequency Comparator Model 100. The field site standard could be set to the same frequency as the ERL primary standard to within  $\pm 0.2$  parts in  $10^{10}$ . (Note Appendix 1.)

If the two 46.55 mhz frequencies which are synthesized from the appropriate standards at each field site were in error by 10 parts in  $10^{+10}$ , a  $2\pi$  radian shift would be produced in both the  $A(t) \sin \phi(t)$  and the  $A(t) \cos \phi(t)$  each 20 seconds. This rate of phase shift was less than 1/10 the magnitude of the rate of phase changes found on the channel. Frequency differences of 10 parts in  $10^{10}$  between the two field site standards were not expected. The effects of frequency differences were not observed during the testing.

### 2.3.3 EQUIPMENT

The Montronics Frequency Synthesizer Model 301 at the Seattle terminal, set for 5.81125 mhz was the input to the transmitter exciter which multiplied the frequency by 8. The 46.55 mhz was then amplified to 20

watts and fed the main transmitter. The transmitter output of 800 watts went to a 6-element Yagi antenna mounted 35' above the ground and directed at Bozeman. When tests were being conducted, the Seattle terminal transmitted a cw signal with a 30-second break each half hour for station identification.

At the Bozeman field site the signals were received on a 6-element Yagi antenna mounted two wavelengths, (36 ft.), above the ground with the antenna directed toward Seattle. As the signals feeding the receiver from the antenna were very low in amplitude (maximum signal levels range from 40 to 150 microvolts) a receiving and quadrature function generating system as shown in Figure 6 was not possible. Leakage and radiation from the  $\sin \omega_0 t$  and  $\cos \omega_0 t$  would more than saturate the receiver. It was necessary to convert the received signal to an intermediate frequency (IF). As a mixing signal was used which was synthesized from the local frequency standard, no information was lost. The only change to the original signal was an amplitude factor K and a change in the carrier radian frequency to  $(\omega_0 - \omega_1)$ . No change had occurred to  $\phi(t)$  due to the translation.

The receiver mixed a 48.80 mhz signal, synthesized with a Montronics Frequency Synthesizer Model 301 from the local frequency standard, with the received signal. The transistor receiver had a noise figure of 3.8 db., a bandwidth of 20 khz, a 0.1  $\mu$ volt sensitivity, and an output IF frequency of 2.25 mhz. The 2.25 mhz IF was mixed with a 2.0 mhz signal synthesized from the Sulzer Model 2.5 frequency standard. The output of this mixer and lowpass filter was a 250 khz signal with 1,000 hz bandwidth. At this stage in detection, the signal was of the

form shown below.

$$K_2 A(t) \cos (2\pi \times 250 \times 10^3 t + \phi(t))$$

The amplitude function  $A(t)$  was simply scaled by  $K_2$  and the phase variation  $\phi(t)$  was unchanged. From this signal the quadrature signals were derived. Circuit element limitations made the quadrature function generation at a higher frequency impractical. The actual quadrature function generation was then as shown in block diagram form below.

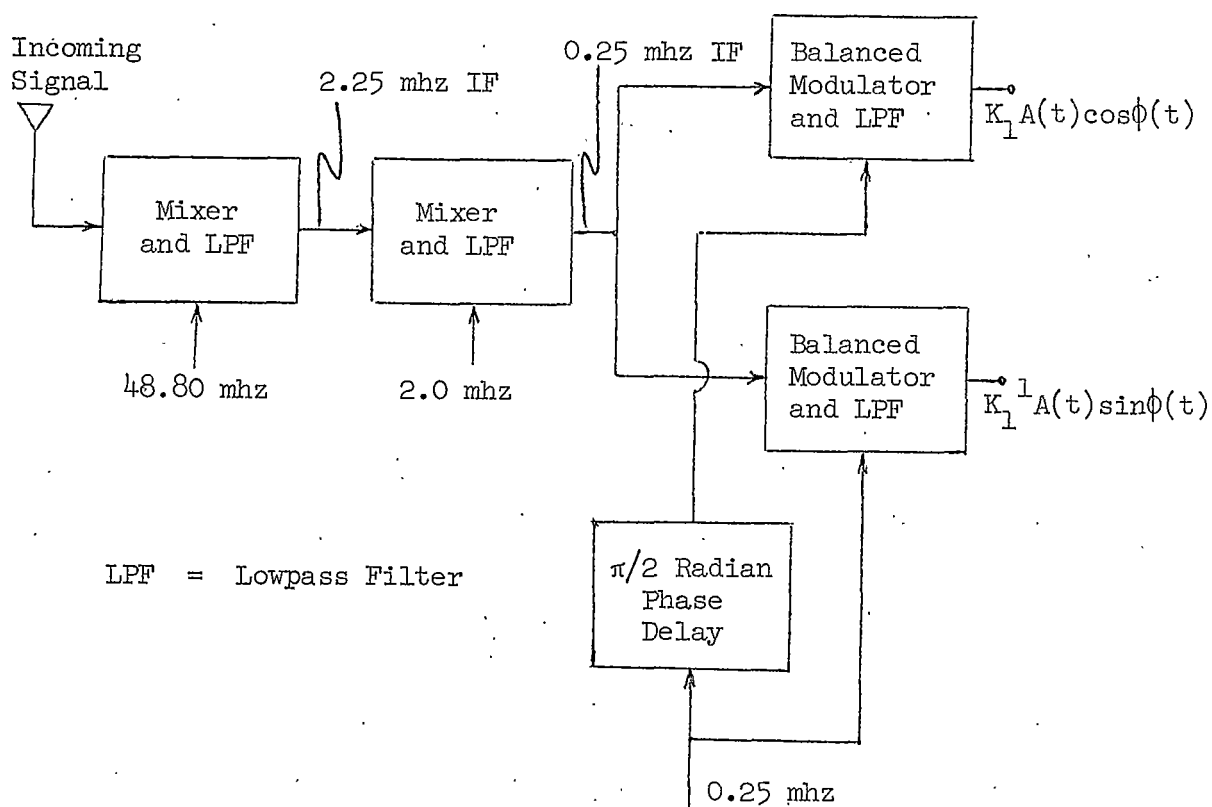


Figure 8.

Functional Block Diagram of Quadrature  
Function Receiving System

The 48.80 mhz, 2.0 mhz, and 0.25 mhz signals were each derived from the Bozeman field site Sulzer frequency standard. The constants  $K_1$  and  $K_2$  were adjusted so that the two output amplitudes were equal in amplitude for a given input. The balanced modulators were unique devices. A detailed discussion of balanced modulators and their outputs is given in D. K. Weaver's thesis.<sup>(79)</sup> The final lowpass filters that the signals passed through had 3 db. bandwidths of 150 hz.

The two quadrature functions and the detected 2.25 mhz IF were recorded on a Brush strip chart recorder. The 3 db pen response was at 60 hz. At 120 hz the response was down 10 db. As the phase variations in quadrature form were, so to speak, folded over the zero frequency, the 3 db bandwidth of the system to frequency shifts around the 46.55 mhz signal was 120 hz while the 10 db response bandwidth was 240 hz. A diagram of the system block components is shown in Figure 9.

#### 2.3.4 QUASI-QUADRATURE FUNCTIONS

The equipment for measuring the phase stability of the vhf meteor trail forward scatter link was operational in early 1964. After several trial runs it was obvious that the detected IF channel was providing all the information needed relative to the amplitude of the received signals. The amplitudes of the quadrature functions were of little value. Then, as each balanced modulator and lowpass filter was an integrating correlator, why not overamplify the received signals--until an input voltage to the receiver of 5 to 10  $\mu$ volts produces a square wave at the input to the balanced modulators? The 250 khz signal from the frequency

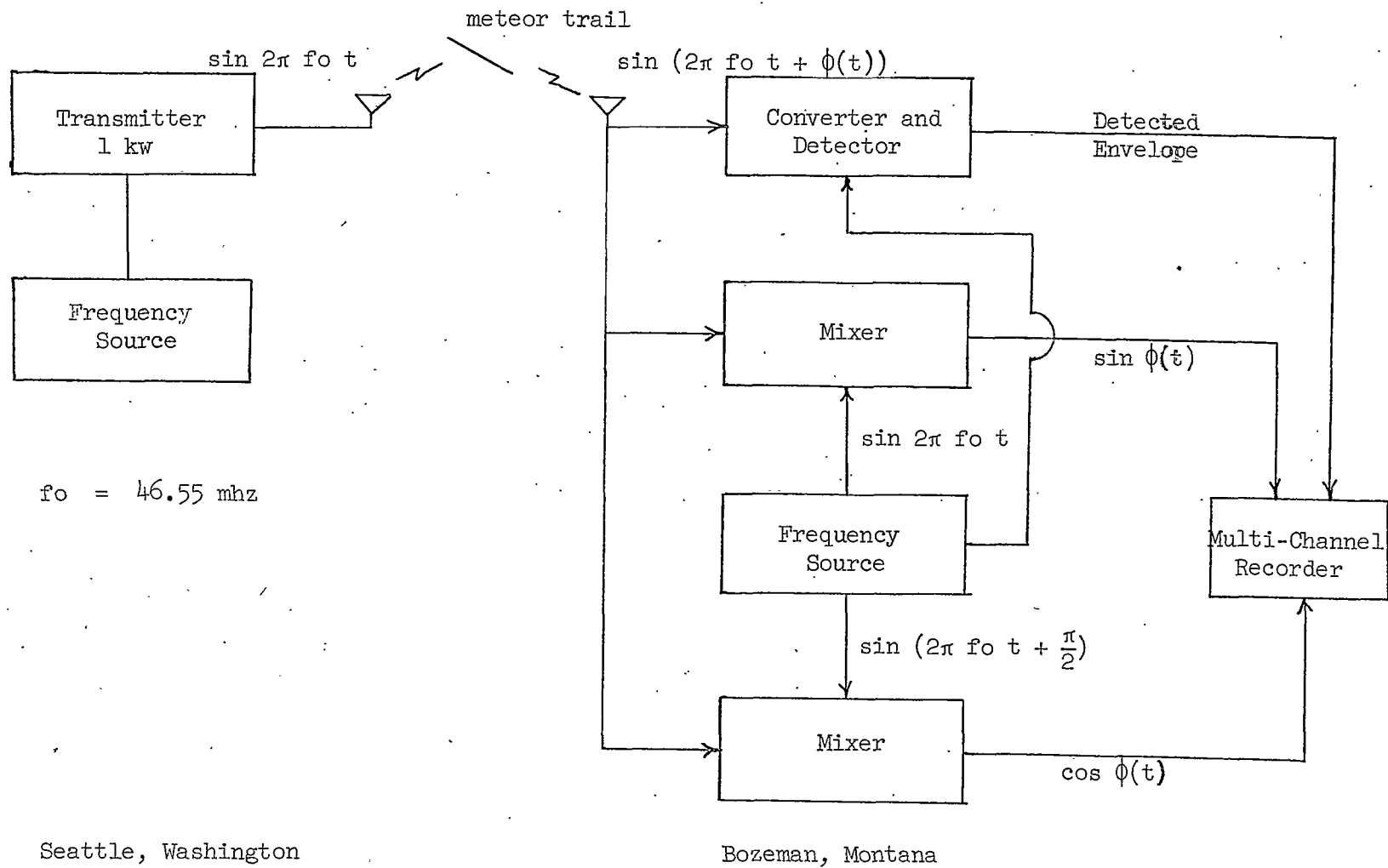


Figure 9. Functional Block Diagram of Phase Stability Measuring System.

standard was already a square wave. With the inputs in this form, the outputs of the balanced modulators were much more sensitive to input signals. The amplitude of the signal into the receiver needed to produce an output from the lowpass filters was approximately  $0.1 \mu$  volt. When a strong signal was present, the lowpass filter outputs increased in amplitude until the input signal reached a  $10 \mu$  volt level. At that input signal level the lowpass filter outputs were at a maximum level such that additional input signal amplitude had no effect on the filter outputs. It was no longer true that for the functions,  $E_1(t)$  and  $E_2(t)$ , that  $A^2(t) = E_1^2(t) + E_2^2(t)$  where  $A(t)$  was the amplitude of the 250 khz IF signal. The phase variations in the  $\sin \phi(t)$  and  $\cos \phi(t)$  portions of the quadrature components remained unchanged. The functions contained all the information that was needed from the quadrature outputs. These amplitude distorted quadrature outputs were called the quasi-quadrature outputs. The individual outputs were labeled  $\sin \Delta\phi$  and  $\cos \Delta\phi$ .

### 2.3.5 CALIBRATION

The only chart calibration for the quasi-quadrature channels was to insure that the maximum pen. excursions stayed on the paper. The detected IF channel was usually calibrated as shown in Figure 10.

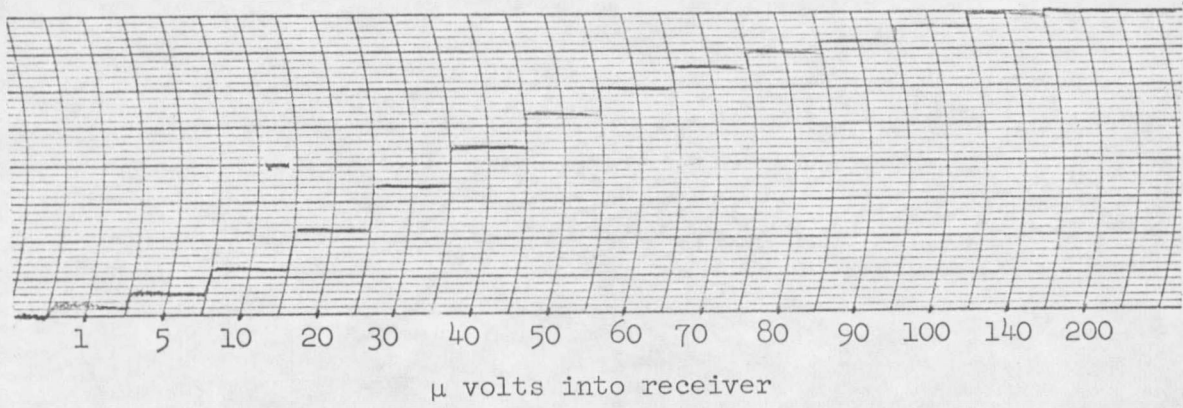


Figure 10.

Detected IF Recording Calibration



### 3.0 DATA ANALYSIS

### 3.0 DATA ANALYSIS

#### 3.1 PROCEDURE

##### 3.1.1 AMPLITUDE CONSIDERATIONS

Each signal whose amplitude exceeded the 3  $\mu$  volt input level was considered in the data analysis. Those signals received below this level were not included in the data analysed. A signal whose amplitude never exceeded the 3  $\mu$  volt input level would not be used for communication with an actual system. Due to the overdriven amplitude in the quasi-quadrature function generating circuitry the phase variations of the low amplitude (less than 3  $\mu$  volt input) signals were well defined. No phase variations were observed for these signals which were not similar to the phase variations of the higher amplitude signals. The phase variations were not a function of the amplitude of the received signal (except for what later will be referred to as early fast doppler).

##### 3.1.2 SHAPE CONSIDERATIONS

The received signals were categorized according to probable reflecting surface type. The three reflecting surface groups were (1) underdense meteor trail, (2) overdense meteor trail, or (3) non-column reflecting surface. In the first group were signals with an initial fast rise time and an exponential decay (note equations 10 and 11). The overdense meteor trail group included those signals with an initial fast rise time that decayed more slowly than an exponential decay. The non-column reflections did not have an initial fast rise time. Some of the latter reflections were from non-meteoric reflecting surfaces such as temperature inversion layers and Sporadic E. (82)

A certain number of the group were from meteor trails not exactly tangent to an ellipsoidal spheroid with the two terminals as foci. Another possibility was that the non-column reflection was from a surface of high electron density blown from an overdense meteor trail. Such a trail was initially oriented such that no reflection was present between the two terminals. There was no apparent way to separate the non-column reflections as to the source of the reflection. The conceptual form that was used for each of the three categories of signals is shown below.

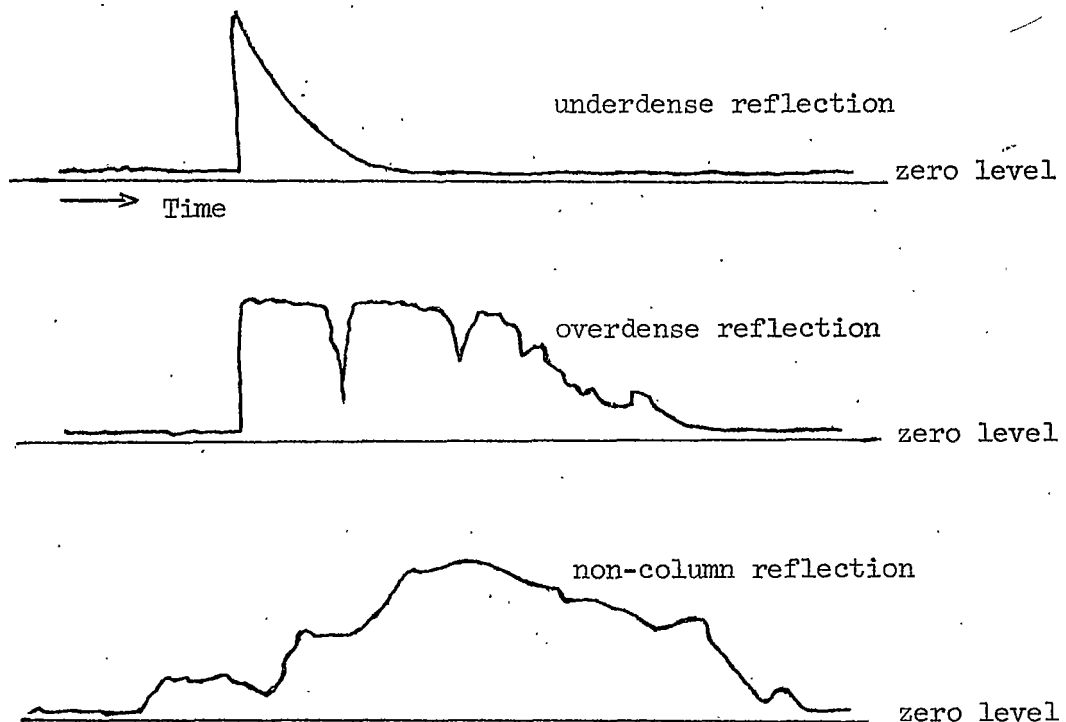


Figure 11.  
Sample Reflection Types

On several occasions low amplitude signals were received that produced nearly perfect sinusoids on the quasi-quadrature outputs for periods of a minute or more. The sinusoidal nature of the  $\sin \phi(t)$  and  $\cos \phi(t)$  terms showed that the path length was changing at a constant rate with respect to time. The signals were constant for such a long period that an ionospheric anomaly was unlikely the cause. A reflection from either a satellite or a high aircraft could have produced such a signal. The phase variations of these signals were always at a low rate. As the signal amplitudes did not exceed the 3  $\mu$ volt threshold, they were not included in the results.

### 3.1.3 SIGNAL PHASE CHANGES

The magnitude of the phase change of a received signal compared to the local signal was determined by measuring the consecutive periods of the quasi-quadrature functions. Initially, quarter cycle measurements were made. This was time consuming and the small increments were found to be unnecessary. Full-cycle measurements were made except where there were phase reversals or a questionable area.

The sign of the phase changes was determined for the signal throughout each reflection. This was determined by noting whether the  $\sin \phi(t)$  term lead  $\cos \phi(t)$  by  $\pi/2$  radians or vice versa. If the path length was shortening at a constant rate the received signal was high in frequency. This produced a positive phase change (i.e., the  $\sin \phi(t)$  term was leading). If the path length was lengthening at a constant rate, then the received signal was low in frequency; the phase change was considered.

negative, and the  $\cos \phi(t)$  term lead.

When the equipment was constructed, the quasi-quadrature channels were not labeled. To determine which quasi-quadrature signal lead under each condition, signals slightly offset in frequency were applied to the receiver input. A 46,550,010 hz signal produced 10 hz sinusoids at the quasi-quadrature outputs with the  $\sin \phi(t)$  term leading by  $\pi/2$  radians. A 46,549,990 hz signal again produced 10 hz sinusoids but with the  $\cos \phi(t)$  term leading. It was also noted that saturating the receiver had no effect on the quasi-quadrature outputs.

### 3.1.4 EXAMPLES

#### 3.1.4.1 UNDERDENSE METEOR TRAIL REFLECTION

In Figure 12 is shown a recording of the detected IF and quasi-quadrature components of an underdense meteor trail reflection. The paper velocity was 25 mm/sec. A plot of the phase change of the received signal versus time is shown in Figure 13.

One cycle of the  $\sin \phi(t)$  term represents  $2\pi$  radians shift of the received signal. If, as in this case the  $\sin \phi(t)$  term is leading, then the path length shortened by 6.42 meters during the  $2\pi$  radian shift. The phase plot with respect to time shown in Figure 13, is, for all practical purposes, a straight line--a linear function of time. Such phase shift is attributed to upper atmospheric winds. (33,34,35,51,73,78) Most meteor trails which produce reflections between Bozeman and Seattle are in the vicinity of the midpoint between the two stations. (49,83) If  $R_1 = R_2 = 500$  km, then a constant velocity movement of the effective reflecting

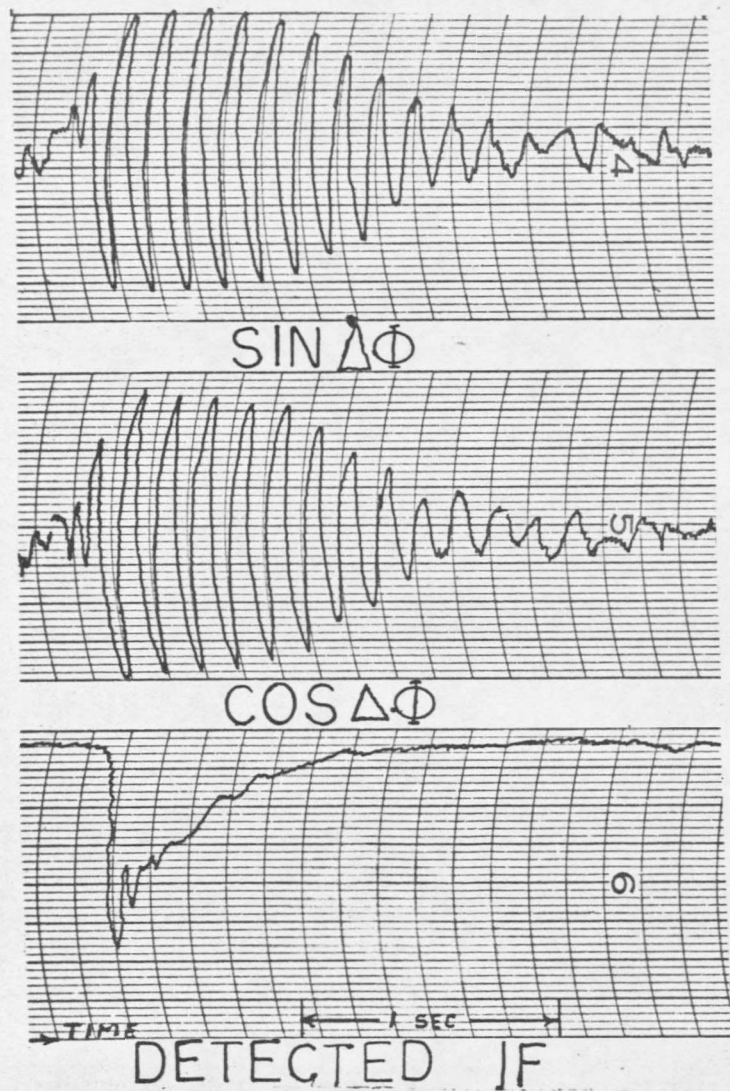


Figure 12. Underdense Trail Reflection

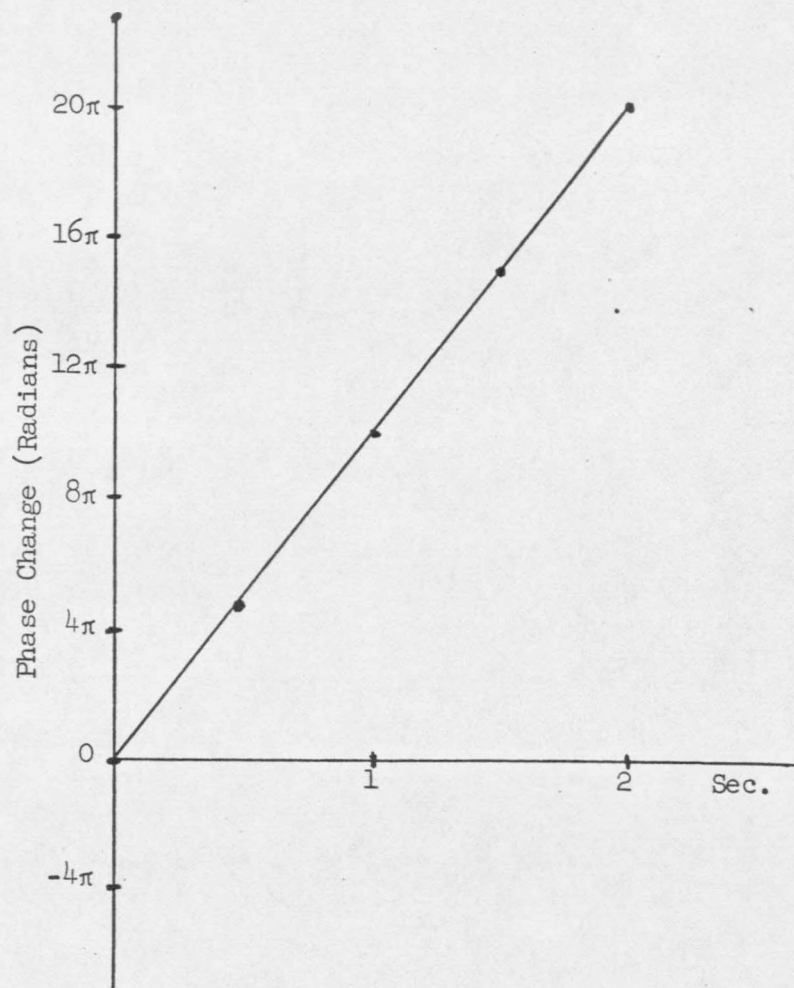


Figure 13. Phase Plot of Underdense Trail Reflection Shown in Figure 12.

point produces a phase variation that is a linear function of time, at least to the accuracies of the recording techniques used. As the movement of the trail is small in comparison to  $R_1$  and  $R_2$ , the geometry remains essentially constant throughout the reflection.

### 3.1.4.2 OVERDENSE METEOR TRAIL REFLECTION

Figure 14 shows the detected IF and two quasi-quadrature functions associated with an overdense meteor trail reflection. The detected IF shows the signal above the noise level for approximately 3 seconds. The quasi-quadrature outputs show the signal phase changes for approximately one second longer. Note that the amplitudes of the quasi-quadrature outputs are almost unrelated to the IF detector. To avoid this, the detected IF zero level was offset from the graph paper zero. Again the  $\sin \phi(t)$  and  $\cos \phi(t)$  terms are nearly sinusoidal. As expected, the plot of the change in phase of the received signal with respect to time is nearly a straight line, (note figure 15). The slope of the line increases slightly after 1.25 seconds and is constant for the remaining three seconds. The maximum rate of change of phase with respect to time in this example is less than  $2\pi$  radians/sec while in the last example, the underdense trail, the maximum rate was  $10\pi$  radians/sec. This overdense trail was not blown into separate reflecting areas as there are no sudden fades in the signal level and no abrupt changes in the phase. The path length was decreasing at a constant rate.

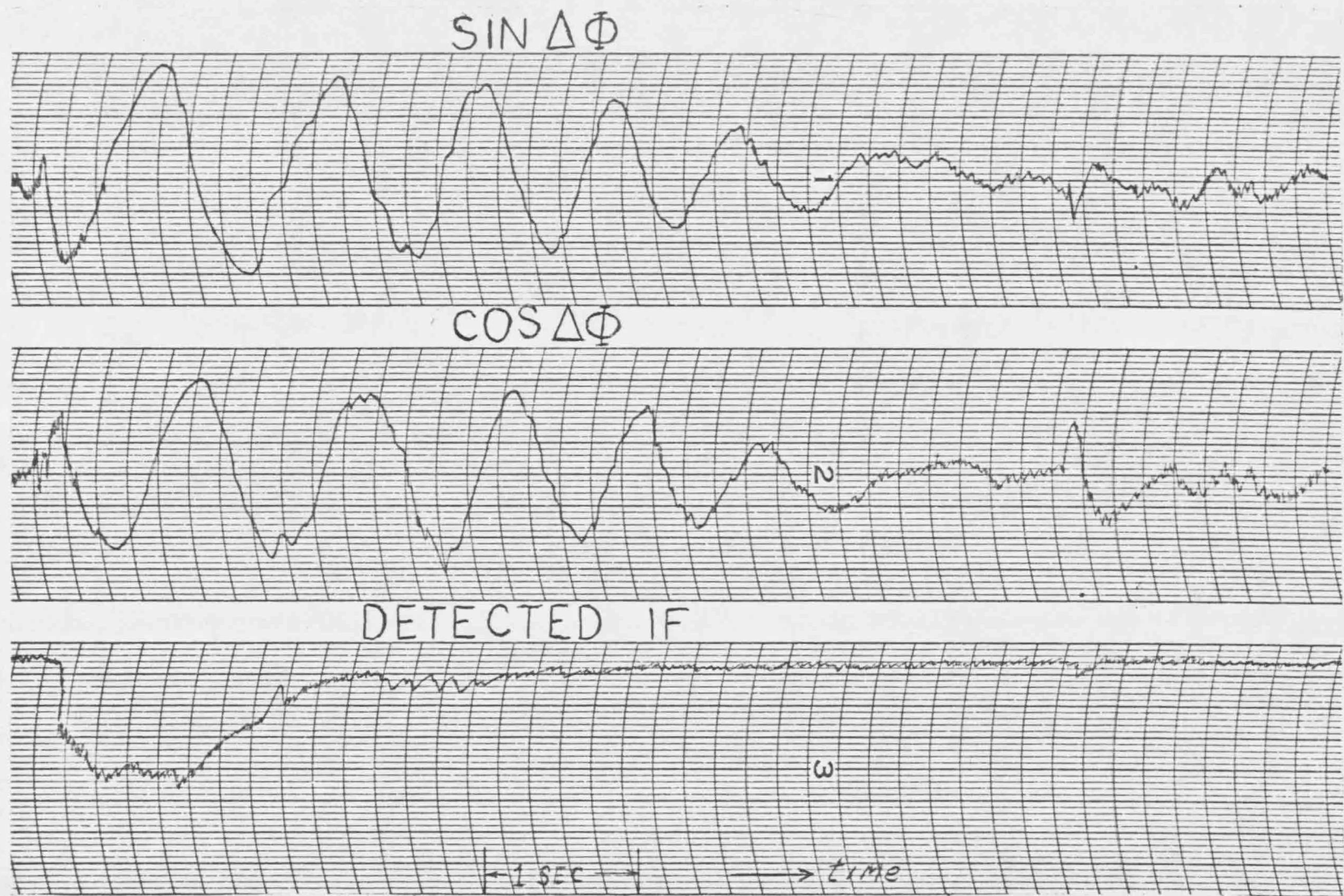


Figure 14. Overdense Meteor Trail Reflection



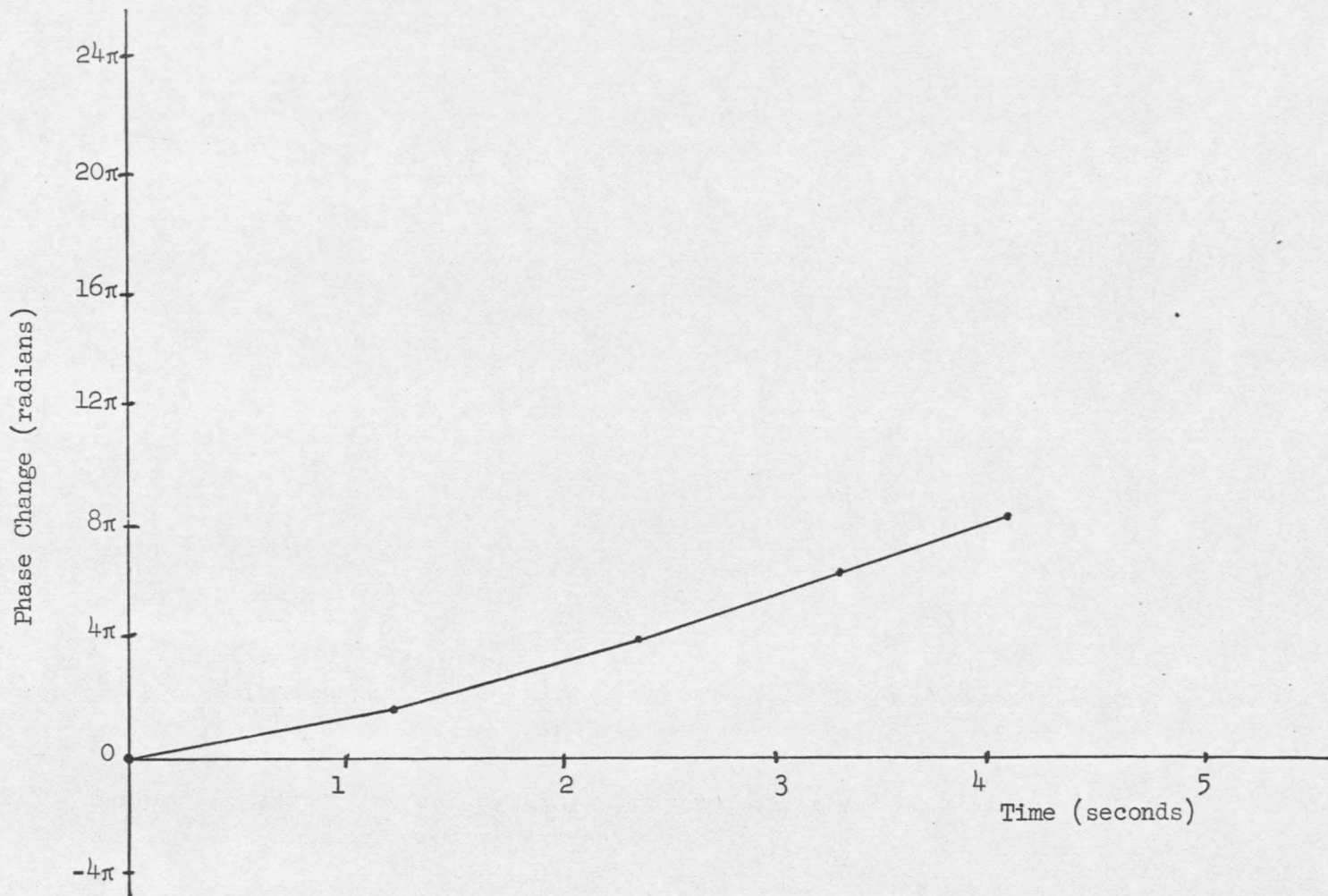


Figure 15. Phase Plot of Overdense Trail Reflection Shown in Figure 14.

### 3.1.4.3 NON-COLUMN REFLECTION

Figure 16 shows the recording of a reflection that was categorized as non-column in nature. The recording shows no sudden initial increase in signal level. The amplitude of the detected IF was so high part of the time that the recording pen was off the paper. When this recording was made, the diode in the IF detector was reversed. Hence the signal zero level is on the other side of the recording channel. The recorder dc amplifier gain was set too high in this example. The pen was off the paper before the receiver saturated. The phase plot with respect to time for this reflection, figure 17, shows the effects of at least two different reflecting areas. Initially, the reflecting surface producing the major contribution of the signal was moving so that the received phase was proceeding negative at a rate of  $8\pi$  radians/sec. The path length was lengthening. Then either a second reflecting surface became the primary source of the reflection or there was an unlikely possibility that the first reflecting area changed directions. From the backscatter experimental work done relative to wind action on meteor trails, (33,34,35,73,78) the second possibility was not likely. During the period from  $T=1$  sec to  $T=2\frac{1}{2}$  sec the path length decreased at a rate  $2 \times 6.42$  m/sec, or equivalently, the phase changed at a rate of  $4\pi$  radians/sec. Note that the slope of the phase plot corresponding to this region is positive. For a few tenths of a second the phase was more positive than when the reflection began. After  $T=2.5$  sec the direction of the phase change direction reversed and again the path length increased at approximately  $8\pi$  radians/sec. This is essentially

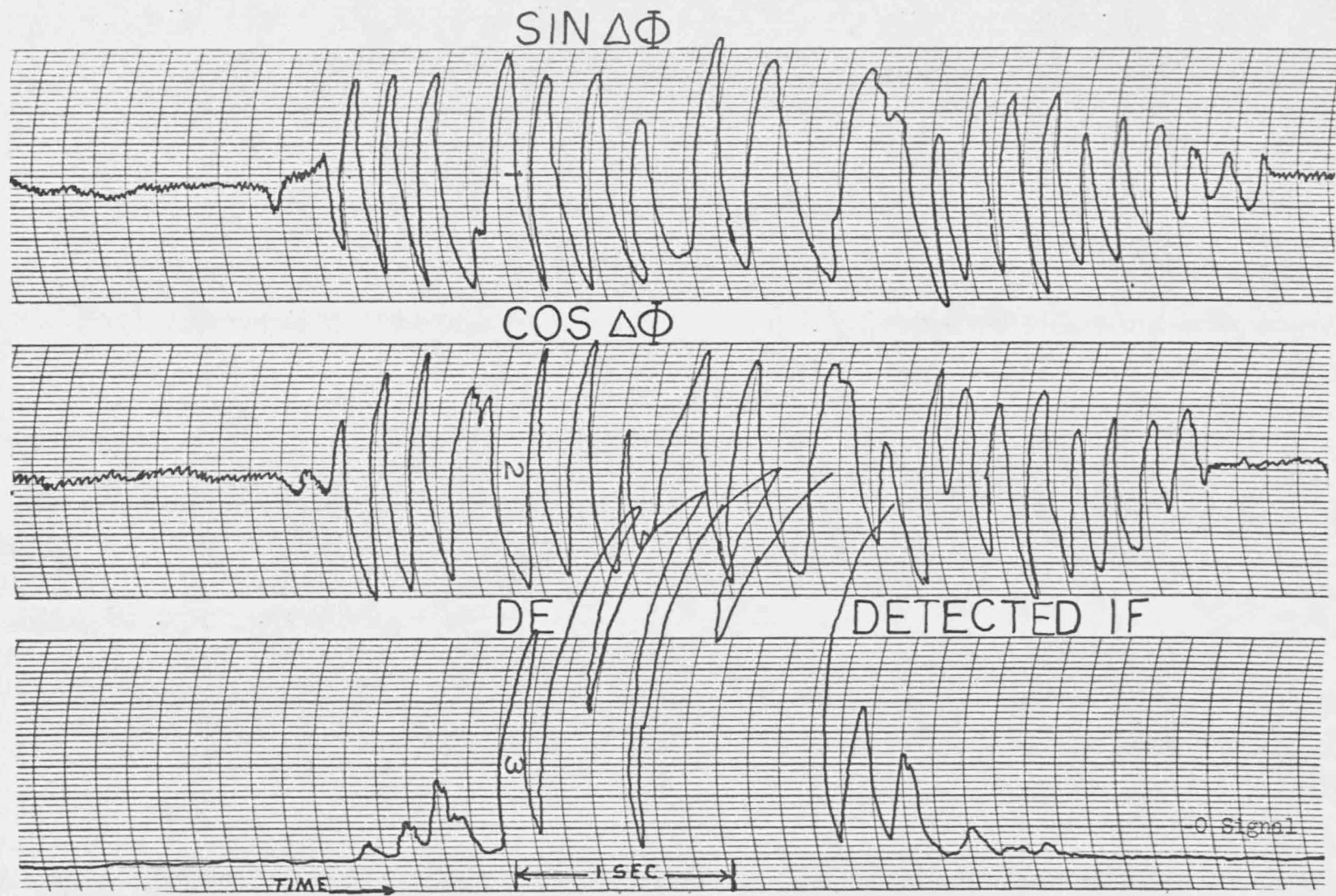


Figure 16. Non-column Reflection

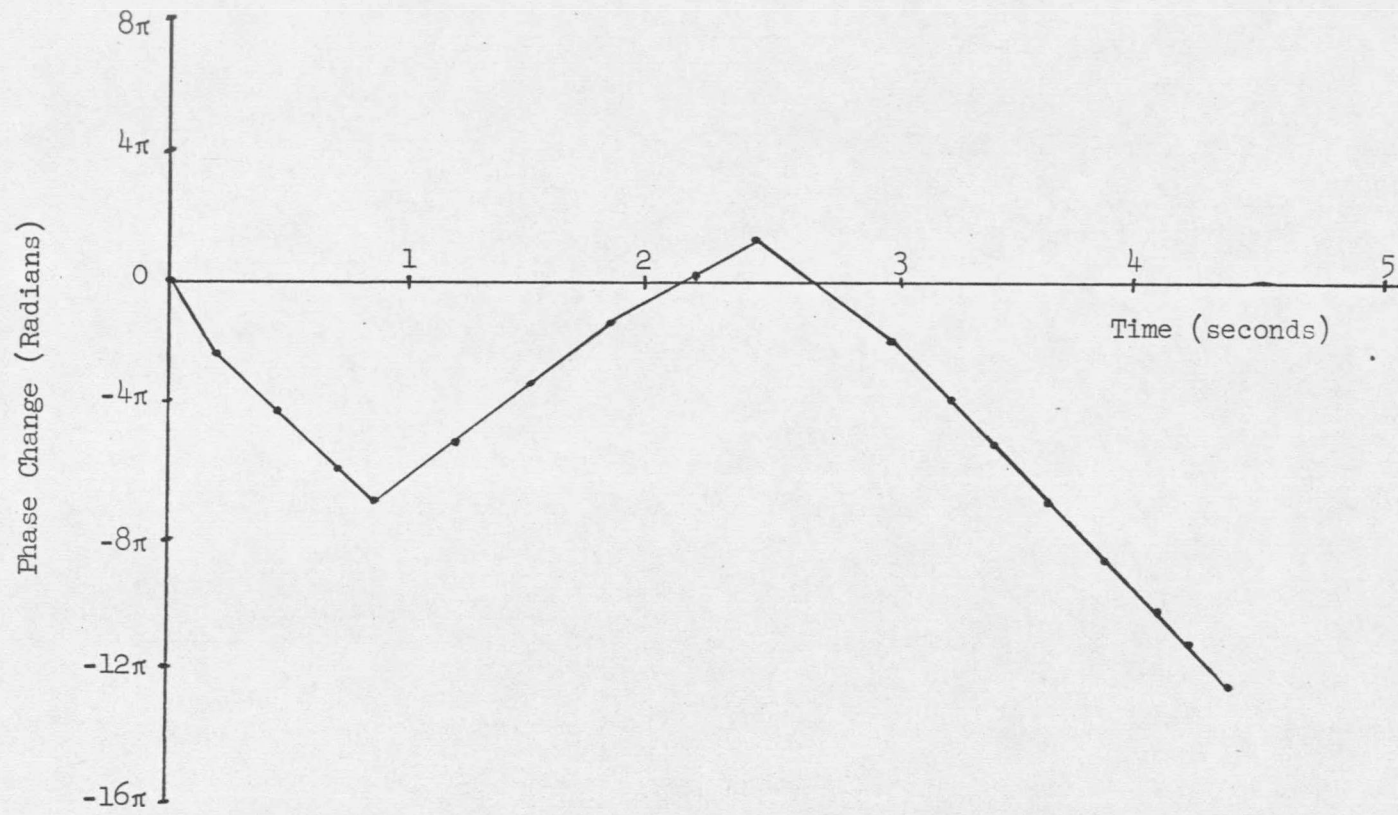


Figure 17. Phase Plot of Non-column Reflection Shown in Figure 16.

the same rate that was present during the first one second of the reflection. Hence the reflection surface present after  $T=2.5$  sec was either the initial reflecting surface or another surface under the same wind influence. The apparent (and not valid) sudden reverses in phase direction as shown in Figure 17 were a result of the manner in which the curve was drawn--a series of straight lines between sample points.

When measuring the phase stability of the reflection from a meteor trail and plotting the phase of the received signal versus time, large errors can be introduced if the measuring and plotting is done as in Figure 17. If a signal is reflected from A to B at time  $t_0$ , its propagation time will be  $\tau_0$ . If some  $\Delta t$  time later a second signal is transmitted, then by simply moving along the time axis a  $\Delta t$  length, the change in phase of the received signal can be measured. From this the value of  $\tau$  at time  $t_0 + \Delta t$  can be calculated. That process isn't true when a second meteor trail affords another path for the signal. In this case it is not possible to determine the change in path length from a phase plot of the received signal. The second path may be longer or shorter than the first. This phenomenon has been discussed here as an exactly similar argument is true relative to the phase plot of Figure 17. The signal primarily responsible for the quasi-quadrature outputs during the first second of the reflection shown in Figure 16 was reflected from an effective reflecting point which was moving at a nearly constant velocity. The channel was lengthened at about  $2 \times 6.42$  feet/sec. After one second, a different reflecting area became predominant. The important question is, "Has the path length changed?" The answer is

"Yes." The reasons will be shown in the interpretation of the results.

### 3.2 OTHER ANALYSIS CONSIDERATIONS

#### 3.2.1 ANALYSIS PROBLEMS

After plotting the phase of the first fifty reflections, several things were apparent. The first was that this process took a long time for each reflection. To carefully measure and plot the phase changes and to note which quasi-quadrature function was leading took on the average 25 to 30 minutes per reflection. At this rate the sample size wasn't going to be very large. To analyze the reflections received during a four-hour recording period during March might take 80 to 100 hours.

Another problem soon arose. If there were 100 phase plots from a particular type of reflection, what was the average change in phase for the group of reflections? Or, more simply, how could 100 phase plots be averaged? Several attempts were made to do this but either the results were meaningless or too many restrictions were needed for the reflections considered.

Also, how were reflections with more than one controlling Fresnel zone present to be considered? The  $2\pi$  radian phase differences between the signals reflected from each area were unknown.

#### 3.2.2 RATE OF CHANGE OF PHASE

To achieve a workable phase measuring system and meaningful averages, a simple method was devised to quantize the data. Most of the reflections had phase changes that were linear functions of time, as

in figures 13 and 15. The slope,  $d\phi/dt$ , described the line in each such case. Each phase plot line started at the origin. If the phase plot was a straight line, then  $d\phi/dt$  was constant. If the phase plot was a series of straight lines, the reflection had several different, yet constant, slopes. The maximum value of the slope described the worst conditions of the phase stability during a reflection. This value would be a "worst case" for the series of straight line phase plots. The largest value of  $d\phi/dt$  represents the fastest rate of change of the phase of the signal reflected from a Fresnel zone. The largest value of  $d\phi/dt$  was recorded for each reflection.

The maximum rate of change of the phase with respect to time as measured in this experiment contains no information about the  $2\pi$  radian phase multiplicity between signals reflected from two controlling Fresnel zones. Many communication systems, including most time sync processes, cannot operate on a channel with such discontinuities of received phase and hence of path time delay. However, this problem was overcome with a "converging" time sync system. This will be defined and discussed in the time sync section. The expected maximum rate of change of phase with respect to time was the parameter which predicted the system's performance.

Note that  $d\phi/dt$  was the radian frequency of the quasi-quadrature functions. In cases where the phase plot was a linear function of time, as in figures 13 and 15, the quasi-quadrature functions were sinusoids, as in figures 12 and 14, respectively. The frequency of the sinusoids was a direct measure of  $d\phi/dt$ . In figure 13 the frequency of the

sinusoid was approximately 5 hz. This is  $5 \times 2\pi$  radians/sec, exactly the slope of the phase plot in figure 14. Then to determine the maximum phase plot slope of a particular reflection, the period of the shortest cycle of a quasi-quadrature output was measured. If  $f$  was the frequency, then  $f = 1/T$  where  $T$  was the shortest period. The maximum rate of phase change was then  $f \times 2\pi$  rad/sec. The sign of the phase shift was determined for the cycle measured using the process described earlier. Some reflections were so short lived that a complete phase shift cycle was not present. In such cases a half cycle or a lesser fractional cycle period was measured.

In summary, each reflection was categorized as being either from an underdense meteor trail, an overdense meteor trail, or from a non-column reflecting surface. The maximum rate of change of phase was determined by measuring the period of the shortest cycle or fractional cycle of the quasi-quadrature output. The sign of the phase shift was also determined. A reflection as shown in figure 12 was listed as from an underdense trail, a maximum rate of change of  $5 \times 2\pi$  rad/sec with a positive sign to indicate the direction of the phase shift. Reflections similar to that shown in figure 16 were categorized as non-column reflections with a negative  $d\phi/dt$  value of  $8\pi$  rad/sec.

### 3.2.3 DATA REDUCERS

After several weeks of analyzing data in this manner, it was obvious that if only the author did the data reduction, time would limit the sample size. By this time the author knew the algorithms necessary to



reduce the recordings to a usable form. Other people were hired to reduce the data according to the algorithms established. The author would explain in detail the various procedures to each person hired. Each week or two the author would work with the "data reducers" to see that no bad habits or invalid short-cuts had been developed.

A recording period of six to eight hours approximately once a month kept the data reducers busy. Data were gathered throughout the school year starting in August 1964 and ending in June 1965.

#### 4.0 RESULTS OF PHASE STABILITY TESTS

#### 4.0 RESULTS OF PHASE STABILITY TESTS

##### 4.1 DATA HISTOGRAMS

The phase stability tests had to be conducted when it was convenient for the Boeing engineers, when ERL personnel could operate the Bozeman terminal, and when the Boeing transmitter and Bozeman receiver weren't operating on another concurrent project. The monthly recordings were not conducted at the same time each month or for the same length of time. Histograms were used to display the data after they were analyzed. There were no outstanding differences between the monthly histograms and at no time during the year were there particularly unique phase variations.

For a summary ERL report published soon after the completion of these tests in 1965,<sup>(86)</sup> a single histogram was used to represent a sampling of each reflection type from the recording period. The same process will be followed in this writing. The November readings had the least number of reflections. The data recorded in the other months were scaled to this sample size. As 127 underdense meteor trail reflections were received in November, the histogram shown in Figure 18 contains 8 times 127 samples. The overdense trail and non-column reflection groups were scaled proportionately in the same manner. Figure 19 is a histogram of the overdense meteor trails versus phase shift and Figure 20 is the histogram showing the non-column reflections. The number of samples in each histogram is 8 times the number received in November.

##### 4.2 NUMERICAL RESULTS

###### 4.2.1 WORST CASE

Histograms 18, 19 and 20 show that the phase stability of signals

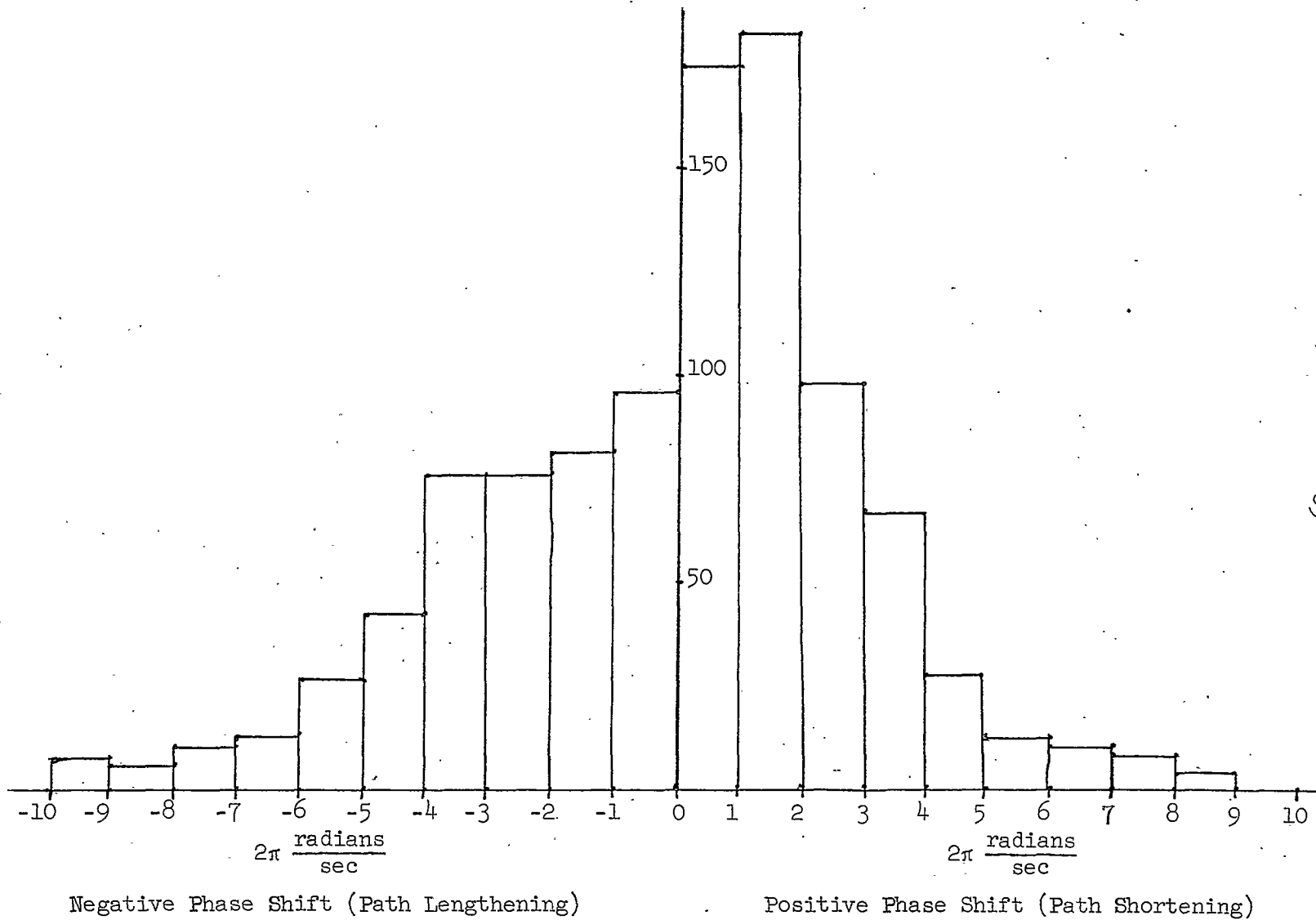


Figure 18. Histogram of 1016 Underdense Meteor Trail Reflections vs. Maximum Phase Shift Rate

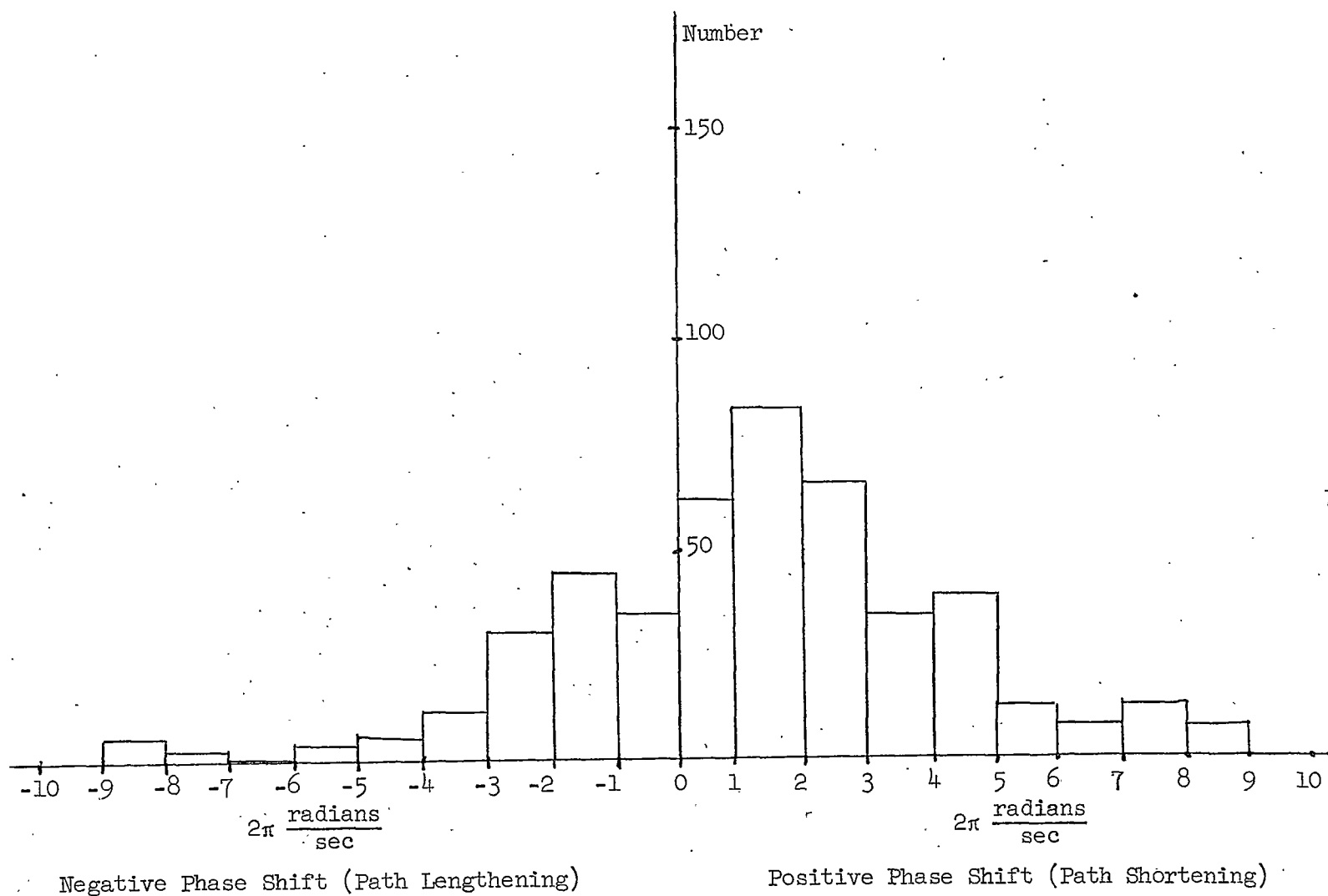


Figure 19. Histogram of 432 Overdense Meteor Trail Reflections vs. Maximum Phase Shift Rate

"# '

G0? @

BN? @@

?

B BD BE B E N \* M  
'(\$ (+ N ) 1 '\$ (+ )  
( 2 ( - U ( +/ + +/V % 2 ( - U ( %' + +/V  
/' C@! %/' (# %- MCD %+B) %\* "#+ - \* ) %+  
2 ! (7 #"# ( - (









































































































































































































